Available online at www.sciencedirect.com
ScienceDirect
Icarus 184 (2006) 344–364
ICARUS
www.elsevier.com/locate/icarus

The primary liquid condensation model and the origin of barred olivine chondrules

M.E. Varela [a,*], G. Kurat [b], E. Zinner [c]

[a] *Complejo Astronómico El Leoncito (CASLEO), Av. España 1512 Sur, CP J5402DSP, San Juan, Argentina*
[b] *Institut für Geologische Wissenschaften, Universität Wien, Althanstrasse 14, A-1090 Vienna, Austria*
[c] *Laboratory for Space Sciences and Physics Department, Washington University, St. Louis, MO 63130, USA*

Received 16 December 2005; revised 27 April 2006

Available online 7 July 2006

Abstract

Barred olivine (BO) chondrules are some of the most striking objects in chondrites. Their ubiquitous presence and peculiar texture caught the attention of researchers and, as a consequence, considerable effort has been expensed on unraveling their origin(s). Here we report on a detailed study of two types of chondrules: the Classic and the Multiple-Plate Type of BO chondrules from the Essebi (CM2), Bishunpur (LL3.1), Acfer 214 (CH3) and DAG 055 (C3-UNGR) chondrites, and discuss the petrographic and chemical data of their major mineral phases and glasses. Glasses occur as mesostasis or as glass inclusions, the latter either enclosed inside the olivine bars (plates) or still connected to the mesostasis. The chemical composition of all glasses, characterized by being Si–Al–Ca-rich and free of alkali elements, is similar to those of the constituents (the building blocks, such as chondrules, aggregates, inclusions, mineral fragments, etc.) of CR and CV3 chondrites. They all have high trace element contents ($\sim 10 \times$ CI) with unfractionated CI-normalized abundances of refractory trace elements and depletions in moderately volatile and volatile elements with respect to the refractory trace elements. The presence of alkali elements (Na + K + Rb) is coupled with a low Ca content and is only observed in those glasses that have behaved as open systems. This result supports the previous finding that Ca was replaced by alkalis (e.g., Na–Ca exchange), presumably through a vapor–solid reaction. The glasses apparently are the quenched liquid from which the olivine plates crystallized. However, they do not show any chemical fractionation that could have resulted from the crystallization of the olivines, but rather have a constant chemical compositions throughout the formation of the chondrule. In a previous contribution we were able to demonstrate the role of these liquids in supporting crystal growth directly from the vapor. Here we extend application of the primary liquid condensation model to formulate a new model for the origin of BO chondrules. The primary liquid condensation model is based on the ability of dust-enriched solar-nebula gas to directly condense into a liquid, provided the gas/dust ratio is sufficiently low. Thus, we propose that chondrules can be formed by condensation of a liquid droplet directly from the solar nebula. The extensive variability in chemical composition of BO chondrules, which ranges from alkali-poor to alkali-rich, can be explained by elemental exchange reactions with the cooling nebula. We calculate the chemical composition of the initial liquid droplet from which BO chondrules could have formed and speculate about the physical and chemical conditions that prevail in the specific regions of the solar nebula that can promote creation of these objects.

Keywords: Cosmochemistry; Solar nebula; Meteorites

1. Introduction

Barred olivine chondrules are considered to be classical droplet chondrules (Dodd, 1978), members of the chondrule family. They consist of a single or of multiple olivine crystals in the form of parallel plates, constituting the Classic or Multiple-Plate Type BO chondrules, respectively. Such chondrules are present in ordinary as well as carbonaceous chondrites. Their spectacular appearance has promoted many efforts to understand their origins (e.g., Lux et al., 1981; McSween, 1977, 1985; Grossman and Wasson, 1983a, 1983b; Weisberg, 1987). The general belief is that these objects were formed by complete melting of solid precursors, followed by supercooling and rapid crystallization (e.g., Nagahara, 1983;

* Corresponding author. Fax: +54 264 4213693.
E-mail addresses: evarela@casleo.gov.ar (M.E. Varela), gero.kurat@univie.ac.at (G. Kurat), ekz@wustl.edu (E. Zinner).

0019-1035/$ – see front matter
doi:10.1016/j.icarus.2006.05.009

Weisberg, 1987; Hewins, 1988, 1989). Such melts need considerable superheating in order to have all memories of the solid precursors destroyed and to crystallize a single olivine from a nucleus that formed in the supercooled melt (as explain in detail in Section 4.2.1). In contrast to this formation model, it has been proposed, that the BO texture can be acquired by rapid growth of subparallel olivine platelets by direct condensation from the vapor followed by subsolidus recrystallization (Kurat, 1988). However, in spite of constant efforts to understand the origin of BO chondrules, there remain two main unresolved problems: the nature of the material from which the chondrule liquids formed and the nature of the heating event.

Kurat et al. (2004) sketched a model of chondrule formation by condensation where these objects can be produced in one single nebular cooling step with the help of the universal liquid (Varela and Kurat, 2004). This simple model answers some of the still open questions concerning the origin of chondrules, as no complex mixing of condensates and re-melting is necessary.

Recently, we have shown the important role that silicate liquids play during the growth of major minerals in the solar nebula (Varela et al., 2005a). This model proposes a liquid-supported condensation process, in which a Si–Al–Ca liquid (the glass precursor) supports the growth of crystals (e.g., olivine, pyroxene, plagioclase) directly from the vapor. Liquids can condense much more easily than crystals because liquids do not discriminate against certain elements and they do not need long-range order—a condition which is very difficult to achieve for a crystal nucleus as several thousands ions have to assemble in the right order within a very short time to create a stable condensation nucleus. Therefore the primary liquid condensation model proposes that the first condensate to appear in the solar nebula is likely to be a liquid. This liquid helps to grow crystals from the vapor similarly to the well-known vapor–liquid–solid growth process (e.g., Givargizov, 1987). That process needs only very small amounts of liquid, which serves as an efficient accommodation site for the condensing species. This model is capable of explaining the mineralogical and chemical variability among most chondritic constituents. However, we can also envision that in the specific regions of the solar nebula where this process occurred, larger quantities than the minimally required amount of liquid could condense, to form droplets. In this way, BO chondrules could have formed directly from the solar nebula. Here we report on detailed studies of some BO chondrules, which allow us to reconstruct their evolution in detail and to show how the primary liquid condensation model can help us to unravel the origin of BO chondrules.

Preliminary results were presented at the Lunar and Planetary Science Conference in Houston, Texas (Varela et al., 2005b).

2. Analytical techniques and samples

Barred olivine chondrules were studied with the optical microscope for the petrographic characteristics of the constituent phases (e.g., glasses, olivines, and pyroxenes) and the occurrences of glass inclusions.

Major-element chemical compositions of constituent phases were obtained with a JEOL 6400 analytical scanning electron microscope (NHM, Vienna) and SX100 and SX50 CAMECA electron microprobes (Institute of Geological Sciences, University of Vienna, Center d'analyses Camparis, Université de Paris V, respectively). Microprobe analyses were performed at 15 keV electron energy and 10 nA sample current. Analyses of minerals and glasses were performed both a focused (∼1 μm) and defocused beam (5 μm). The samples were first analyzed for Na with a counting time of 5 s followed by the analysis of all other elements with a counting time of 10 s in order to prevent premature Na loss from glasses. Basaltic and trachytic glasses (ALV 981 R24 and CFA 47; Métrich and Clocchiatti, 1989) were analyzed as standards and the on-line ZAF program was used for corrections.

Trace element analyses of glasses and pyroxene were made with the Cameca IMS 3F ion microprobe at Washington University, St. Louis, following a modified procedure of Zinner and Crozaz (1986).

The studied chondrules are located in the Polished Thin Sections (PTS) "Essebi," "Bishunpur v. G3684 (2)," "Acfer 214 Algerien," and "DAG055" (all from the NHM, Vienna).

3. Results

3.1. Petrography and chemical composition of phases in BO chondrules

3.1.1. Chondrule Ess-BO-1

This BO chondrule from the Essebi CM2 chondrite (PTS Essebi, NHM, Vienna) belongs to the *Classic Type* as defined by Weisberg (1987). The parallel thin plates of olivine are set into a clear glassy mesostasis and have—as the thin enveloping olivine crust—uniform extinction (Fig. 1). Clear glass inclusions and neck inclusions (glass inclusions still connected to the mesostasis glass) are present in several of the olivine plates (Fig. 1b). The olivine crust has variable thickness, a rough and in places botryoidal surface and irregularly distributed metal inclusions (Ni: 4.3–5 wt%). In places two rims are discernible, one inner, clear one and an outer one that is dusted with metal and features protrusions toward the chondrite matrix.

The chemical composition of all glasses (glass inclusions, neck inclusions, and the clear glassy mesostasis) in Ess-BO-1 is uniformly Si–Al–Ca-rich (Table 1, Figs. 1d and 1e). Olivines have relatively constant FeO contents around 0.74 wt% with a mean of 13 olivine laths (selected from the profile 1–13, white line in Fig. 1a) having 0.8 wt% FeO [Ol. (13), Table 2]. Only one olivine lath located near the surface of the chondrule shows a higher content (FeO: 2.21 wt%). Three small subhedral Ca-rich pyroxenes <30 μm in length and 15 μm wide are present in Ess-BO-1. One is shown by an arrows in Fig. 1c (Table 2), the second is covering an olivine lath, and the third fills interstitial space.

3.1.2. Chondrule Bishunpur Ch-C

This chondrule from the Bishunpur LL3.1 chondrite [PTS Bishunpur v. G3684 (2), NHM, Vienna] is a small, slightly

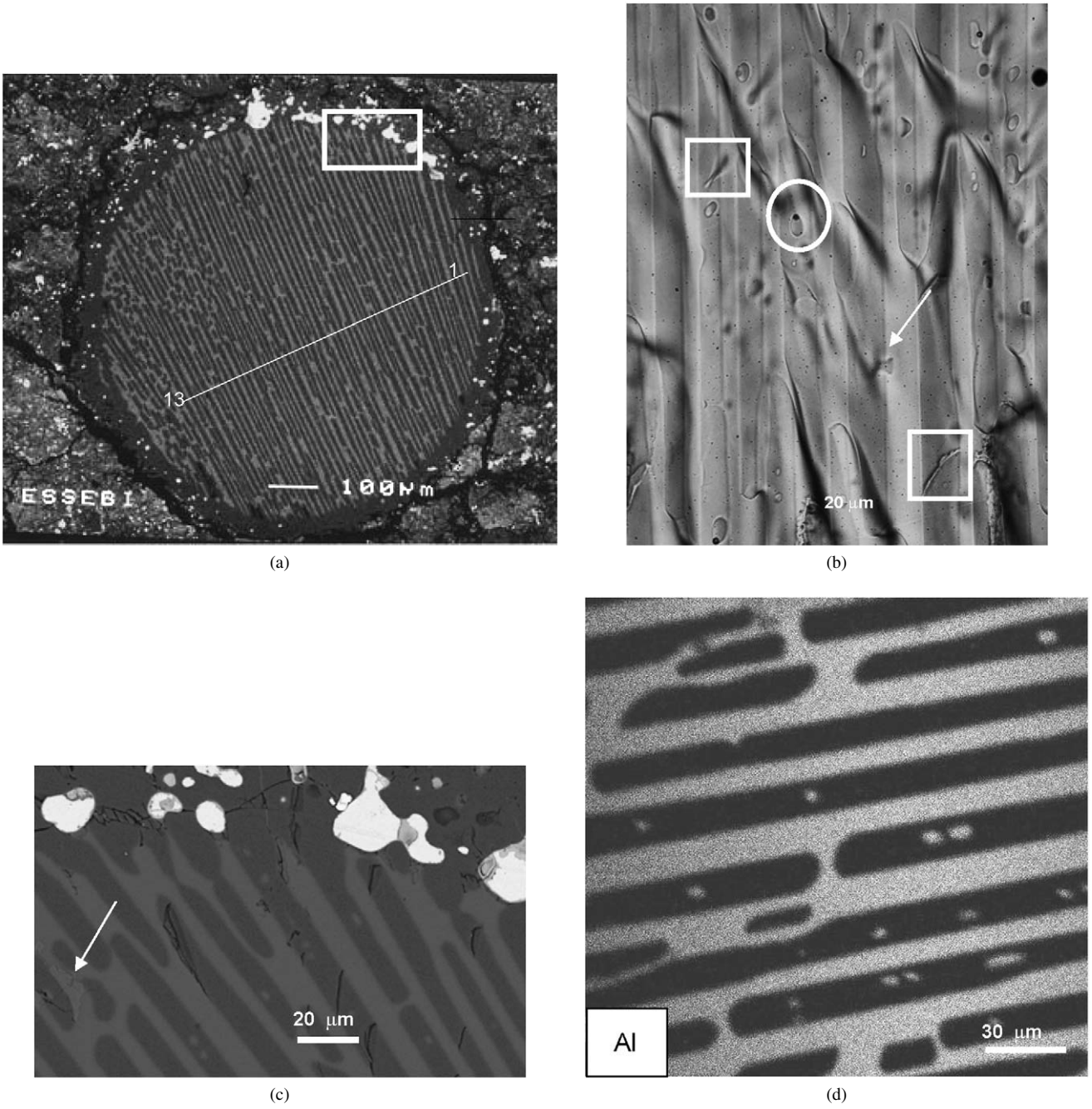

(a) (b) (c) (d)

Fig. 1. (a) Back-scattered electron (BSE) image of BO chondrule Ess-BO-1 (PTS Essebi). The white line (1–13) indicates a traverse along which 13 analyses of olivine plates were made. (b) Transmitted light image of Ess-BO-1 showing the co-existence of glass inclusions (circle), neck inclusions (squares) and the glassy mesostasis (arrows). (c) A detail of the chondrule [rectangular area in part (a)]. (d) Secondary Electron Microscope (SEM) Al image showing the Al-rich composition of the mesostasis and the glass inclusions in olivine. (e) SEM Ca image showing the Ca-rich composition of the mesostasis and glass inclusions in olivine.

oval object of 400 μm in diameter with discontinuous subhedral olivine bars (10 to 30 μm in width), surrounded by a 30 to 60 μm thick olivine shell (Fig. 2a). Glass inclusions—located in the center of the olivine bars—as well as the mesostasis are composed of clear glass (circles in Fig. 2b). An inner rim, speckled with small oxide inclusions, is covered by an FeO-rich rim that carries abundant large oxides. It is tightly intergrown with the inner rim and has a rough outer surface with abundant protrusions into the chondrite matrix. The Bishunpur Ch-C chondrule has no pyroxene. Glass inclusions and mesostasis are Si–Al–Ca-rich with Ca/Al ratios around the chondritic value. Alkalis are present only in the glassy mesostasis in fairly constant amounts, as shown in the ten-step scan profile between two olivine laths [M.G. (10), Table 1]. Olivines in the Bishunpur CH-C chondrule have also very uniform compositions. All olivine laths have a total range in FeO of 1.18 to 1.62 wt% [Ol. Lath (4) is the mean value of a four-step scan profile across an olivine lath, Table 2]. The olivine shell has a fairly constant FeO

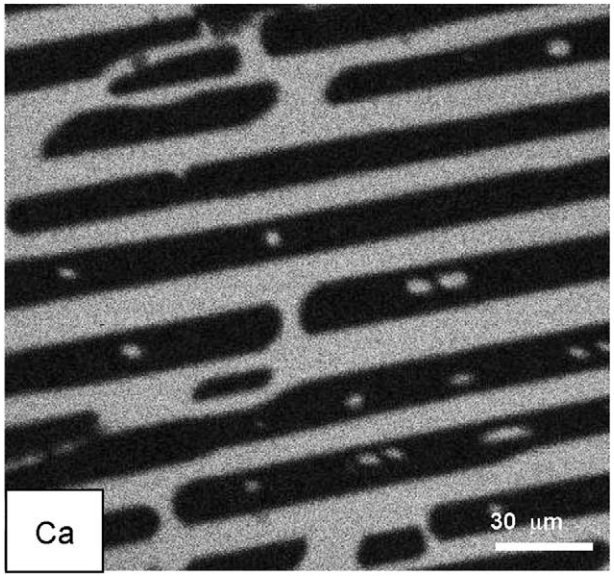

(e)

Fig. 1. (*continued*)

content varying from 2 to 2.45 wt% [Ol. Mantle (4): is the mean value of a four-step scan profile across the mantle olivine, Table 2]. The FeO content of the mantle olivine increases toward the surface of the chondrule (FeO: 7.9 wt%, Ol Mantle B., Table 2).

3.1.3. Chondrule Bishunpur Ch-A

From the Bishunpur LL3.1 chondrite [PTS Bishunpur v. G3684 (2), NHM, Vienna] is composed of two olivine crystals which form a core and a thick mantle (Fig. 3a). The core of this pear-shaped chondrule consists of euhedral to subhedral discontinuous olivine plates and clear glassy mesostasis. The thick mantle consists almost exclusively of olivine in two optical orientations. One of them follows the orientation of the majority of the olivine plates and crystals of the core (Fig. 3b). One core olivine has a glassy neck inclusion (circle in Fig. 3a) and the mantle olivine contains several clear primary glass inclusions (circle in Fig. 3c and inset), some glass pockets, and rounded to subrounded former metal-rich inclusions, now altered to Fe–Ni oxides. Inclusion glasses in the mantle olivine (Fig. 3c) are Si–Al–Ca-rich with no detectable Na and with a chondritic Ca/Al ratio. Glasses from the neck inclusion and the mesostasis are also Si–Al–Ca-rich (Figs. 3d and 3e), with subchondritic Ca/Al ratios and Na_2O contents of around 4.8 wt%. Two step-scan profiles (of seven and five steps, respectively) across the glassy mesostasis show that the glass has a fairly constant chemical composition with Na_2O varying from 4.36 to 4.96 wt%; MgO from 4.7 to 5.8 wt%; FeO from 0.74 to 1.43 wt%; CaO from 11.4 to 12.7 wt%; and Al_2O_3 from 16.4 to 17.3 wt%. The average values of the seven-step scan analyses in the mesostasis [M.G. (7)] are given in Table 1. Olivines in the Bishunpur CH-A chondrule are chemically homogeneous, no chemical variation was detected between the olivine laths and the mantle olivines

Table 1
Major element contents (wt%) of matrix glasses and glass inclusions in barred olivine chondrules (EMP data)

Sample	Ess-BO-1				Bishunpur Ch-C			Bishunpur Ch-A		
	G.I.	N. Incl.	M.G.	M.G.	G.I.	M.G.	M.G. (10)	G.I.	N. Incl.	M.G. (7)
SiO_2	52.6	54.6	53.1	54.4	53.3	51.8	51.2	45.1	59.2	58.7
TiO_2	0.98	1.23	1.00	0.97	0.94	1.04	0.96	1.05	0.73	0.54
Al_2O_3	23.6	19.6	23.3	22.7	20.5	20.2	19.6	28.4	17.8	16.8
Cr_2O_3	0.27	0.32	0.42	0.39	0.35	0.44	0.47	0.27	0.80	0.52
FeO	0.26		0.32	0.35	0.63	0.68	0.59	0.44	0.44	0.95
MnO	0.01	0.03	0.06	0.05	0.02	0.02	0.03	<0.02	0.04	0.05
MgO	4.58	3.30	3.95	3.83	4.92	3.77	4.70	4.23	4.27	5.3
CaO	17.6	20.8	17.4	17.2	18.7	18.4	18.1	20.5	11.0	12.0
Na_2O	0.02	<0.02	0.25	0.20	0.05	2.39	2.38	<0.02	4.89	4.70
K_2O						0.02	0.02			0.2
Total	99.92	99.90	99.80	100.09	99.41	98.76	98.05	99.99	99.17	99.76
Sample	Ac-BO-214/3				Ac-BO-214/4			DAG 055 BO-1		
	G.I.	M.G.	M.G.	M.G.	G.I.	M.G.	M.G.	Ch.M1	Ch.M2	Ap.M.
SiO_2	59.7	50.5	52.0	53.6	58.8	50.2	48.9	48.7	48.3	48.5
TiO_2	0.47	0.60	0.54	0.53	0.47	0.29	0.43	0.04	0.05	0.06
Al_2O_3	16.0	20.6	22.1	20.1	18.2	22.7	23.0	32.2	32.5	32.4
Cr_2O_3	0.41	0.31	0.24	0.35	0.66	0.45	0.25	0.03	0.04	0.04
FeO	0.18	2.51	2.00	2.32	0.16	2.46	2.55	0.46	0.45	0.73
MnO	<0.02	0.04	0.02	0.06	0.02	<0.02	0.04	0	0.04	0
MgO	6.6	4.57	3.81	3.79	1.26	3.36	3.87	0.45	0.31	0.56
CaO	10.6	7.8	5.9	6.9	14.0	5.9	6.6	16.3	16.5	15.8
Na_2O	5.7	12.1	12.4	11.0	6.3	13.0	12.8	2.40	2.25	2.47
K_2O	0.02	1.04	1.08	1.17	<0.02	1.14	1.08	0.04	0.02	0.03
Total	99.67	100.09	100.04	99.82	99.90	99.52	99.51	100.62	100.46	100.59

References. G.I.: glass inclusion; N. Incl.: neck inclusion; M.G.: mesostasis glass; M.G. (10): ten-step scan profile in mesostasis; Ch.M1: chondrule mesostasis; Ap.M.: appendix mesostasis.

Table 2
Major element contents (wt%) of olivine and pyroxene in barred olivine chondrules (BMP data)

Sample	Ess-BO-1				Bishunpur Ch-C			
	Ol. Lath	Ol. Lath	Ol. (13)	Px.	Ol. H. (G.I.)	Ol. Lath (4)	Ol. Mantle (4)	Ol. Mantle B.
SiO_2	42.5	41.5	42.2	49.4	41.3	41.8	41.4	40.5
TiO_2	0.10	0.06	0.08	0.91	0.01	0.04	0.03	<0.02
Al_2O_3	0.07	0.30	0.17	13.8	0.06	0.29	0.07	0.03
Cr_2O_3	0.29	0.29	0.29	0.93	0.23	0.23	0.18	0.09
FeO	0.74	2.21	0.80	0.30	1.19	1.41	2.13	7.9
MnO	0.05	0.04	0.04	0.14	0.03	0.04	0.05	0.32
MgO	56.2	54.5	55.9	15.2	57.0	55.7	55.8	51.2
CaO	0.30	0.3	0.30	18.5	0.29	0.43	0.28	0.16
Na_2O				0.04				
Total	100.25	99.20	99.78	99.22	100.11	99.94	99.94	100.20

Sample	Bishunpur Ch-A				Ac-BO-214/3					
	Ol. H. (N-Incl.)	Ol. Lath (9)	Ol. Mantle (21)	Ol. Mantle B.	Ol. Lath C. (5)	Ol. Lath B.	Px. Crystal (6)	Px. Crystal B.	Px. Mantle (6)	Px. Mantle B.
SiO_2	41.8	42.0	42.6	41.7	42.2	41.6	56.4	50.3	52.6	47.6
TiO_2	0.02	0.03	0.03	0.03	0.05	0.04	0.48	0.90	0.31	1.16
Al_2O_3	0.06	0.09	0.21	0.21	0.40	0.04	3.09	8.3	1.82	11.9
Cr_2O_3	0.24	0.23	0.19	0.19	0.12	0.16	0.67	0.79	0.68	0.97
FeO	0.90	0.86	0.76	1.23	0.73	1.02	0.00	0.22	1.07	0.44
MnO	0.02	0.02	0.02	0.02	0.16	0.11	0.10	0.12	0.20	0.30
MgO	56.6	56.6	55.9	56.6	55.8	56.8	36.7	19.6	41.4	17.3
CaO	0.22	0.23	0.31	0.32	0.24	0.20	2.09	19.9	1.84	20.2
Na_2O								0.03		0.07
Total	99.86	100.06	100.02	100.30	99.70	99.97	99.53	100.16	99.92	99.94

Sample	Ac-BO-214/4					DAG 055 BO-1			
	Ol. Lath (3)	Ol. Lath (5)	Ol. Mantle (7)	Ol. Mantle B.	Px.	Ol. Lath (10)	Ol. Lath (6)	Ch. Px.	Ap. Px. (5)
SiO_2	41.8	41.7	41.6	46.5	48.0	38.8	41.1	51.8	54.4
TiO_2	0.02	<0.02	0.03	0.04	1.35	0.08	0.07	2.44	0.92
Al_2O_3	0.04	0.05	0.16	0.40	11.0	0.28	0.13	3.82	4.25
Cr_2O_3	0.25	0.12	0.30	0.88	0.87	0.21	0.17	0.80	0.71
FeO	1.19	1.35	1.47	2.32	0.41	17.9	5.22	0.69	3.00
MnO	0.06	0.05	0.09	0.17	0.02	0.16	0.10	0.14	0.16
MgO	56.3	56.4	56.2	49.5	17.7	42.1	52.9	19.9	29.4
CaO	0.31	0.22	0.16	0.28	20.6	0.29	0.26	20.5	7.0
Na_2O	0.02							0.05	0.21
Total	99.99	99.89	100.01	100.09	99.95	99.82	99.95	100.14	100.00

References. Ol. (13): mean composition of 13 olivine laths; Px: pyroxene crystal; Ol. H. (G.I.): host olivine of a glass inclusions, Ol. Lath (4): mean composition of a four-step scan profile; Ol. Mantle (4): mean composition of a four-step scan profile in the mantle olivine; Ol. Mantle B.: point analyze at the mantle surface; Ol. H. (N. Incl): olivine host of a neck inclusion; Ol. Lath B.: point analysis at the olivine lath's border; Px. Crystal (6): mean value of a six-step scan profile in the pyroxene; Px. Crystal B.: point analysis at the pyroxene surface; Px. Mantle B.: point analysis at the surface of the mantle pyroxene; Ch. Px.: chondrule pyroxene; Ap. Px.: appendix pyroxene.

(see average of a nine-step scan analysis of an olivine lath from the core and the twenty-one-step analysis from the mantle [Ol. Lath (9) and Ol. Mantle (21), Table 2]), except for the Al_2O_3 and CaO, which are higher, and the Cr_2O_3, which is lower in the mantle olivine than in the central olivine plates. The total range in the FeO content is from 0.6 to 1.2 wt%, with the high value encountered near the surface of the mantle olivine (Ol Mantle B., Table 2).

3.1.4. Chondrule Ac-BO-214/3

This chondrule from the Acfer 214 chondrite (PTS Acfer 214 Algerien, NHM, Vienna) belongs to the *Classic Type* (Fig. 4). The parallel plates of olivine have clear glass inclusions and neck inclusions and are set into a clear glass mesostasis (Fig. 4b). The Ac-BO-214/3 chondrule is enveloped by a thin (∼50 μm) pyroxene crust. Euhedral to subhedral pyroxenes, up to 250 μm in size, are present inside the chondrule (Figs. 4a and 4b). They show crystal faces against the glass and complex grain boundaries with olivine. The olivine laths become thinner where pyroxene appears and diminish inside pyroxene. The olivine plate in contact with the border of the pyroxene crystal show a series of parallel straight-line glass inclusions in the center of the plate parallel to the olivine plate (thin arrow in the SEM Al image, Fig. 4c). The surface of the olivine lath close to the pyroxene is retracting toward the center of the original plate (see SEM Al image, Fig. 4c). A second olivine plate forms a wedge where overgrown by the pyroxene. The olivine lath becomes thinner from the border (high-Ca) to the center (low-Ca) of the pyroxene crystal where it terminates. The decrease in thickness of this wedge is well visible in the

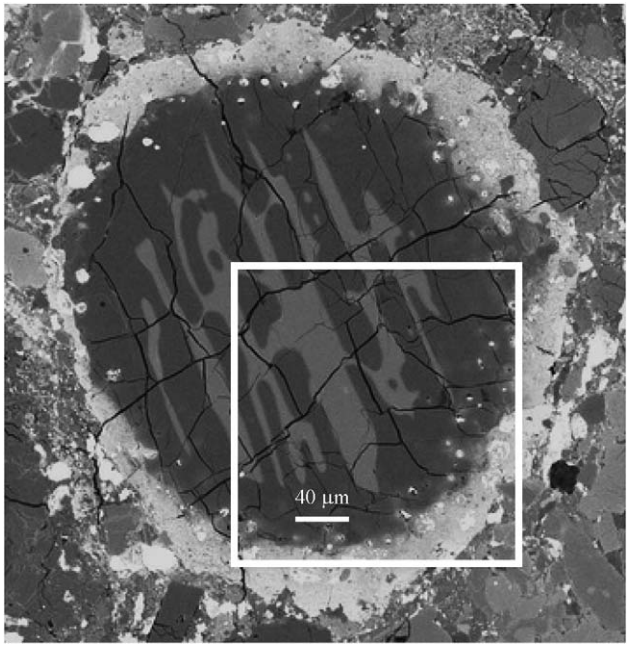

(a)

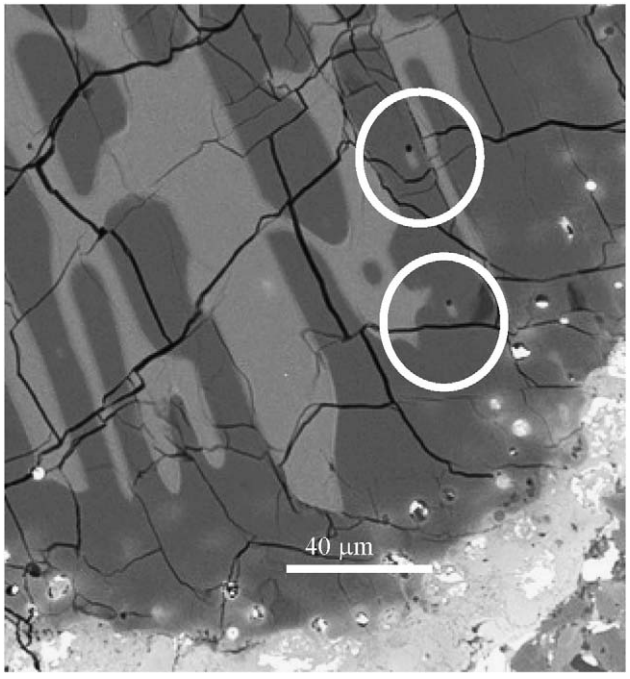

(b)

Fig. 2. (a) BSE image of the Bishunpur CH-C chondrule (PTS Bishunpur v. G3684). (b) Detail BSE image [rectangle in part (a)], showing location of the glass inclusions in olivine (circles).

SEM Mg image (Fig. 4d). The chondrule has also large voids (Fig. 4a).

The clear glasses of inclusions and mesostasis are Si–Al-rich but have lower Ca contents (Table 1) than in Ess-BO-1. All glasses in this chondrule are alkali-rich, with Na_2O and (K_2O) contents varying from 5.7 wt% and (0 wt%) in glass inclusions to 12.4 wt% and (1.17 wt%) in the mesostasis, respectively. Chemical compositions of all olivine laths are similar to each other. Only a slight change in the FeO content is observed from the olivine laths located in the center of the chondrule [Ol. Lath C (5): 0.73 wt% FeO] to those located near the surface of the chondrule (Ol. Lath B: 1 wt% FeO, Table 2). The Al_2O_3 content, however, falls in this sequence from 0.4 to 0.04 wt%. The chemical compositions of low-Ca pyroxenes forming the enveloping crust of the chondrule [Px. Mantle (6): mean value of a six-step scan profile in the pyroxene crust] and those forming the subhedral to euhedral crystals inside the chondrule [Px. Crystal (6): mean value of a six-step scan profile in the pyroxene crystal] are similar, except for FeO and (Al_2O_3), which vary from 0.00 and (3.09) wt% in the Px. Crystal (6) to 1.07 and (1.82) wt% in the Px. Mantle (6) (Table 2). High-Ca pyroxenes (thick arrow in Fig. 4b) are present around low-Ca pyroxene crystals (thin arrow in Fig. 4b) and in the inner surface of the pyroxene crust (Figs. 4b and 4e). All high-Ca pyroxenes have a similar chemical composition (Px. Crystal B. and Px. Mantle B., Table 2).

3.1.5. Chondrule Ac-BO- 214/4

This chondrule from the Acfer 214 chondrite (PTS Acfer 214 Algerien, NHM, Vienna) contains groups of olivine plates oriented in different directions (Fig. 5) and is enveloped by a thin (<50 μm) olivine crust. Clear glass inclusions are located in the center of the olivine laths (arrows in Fig. 5b) which are set in a clear glassy mesostasis. Voids are common, many have smooth outlines and mainly replace the glassy mesostasis (Fig. 5c).

The chemical composition of glasses in Ac-BO-214/4 are Si-, Al-, and alkali-rich with Na_2O contents of 6.3 and 13 wt% in glass inclusions and mesostasis, respectively, and K_2O contents reaching 1.14 wt% in the glassy mesostasis. The olivine laths have FeO contents [Ol. Lath (3): 1.19 wt% and Ol. Lath (5): 1.35 wt%, Table 2] similar to those of the olivine that forms the mantle [Ol Mantle (7): 1.47 wt%, Table 2]. A slight increase in the FeO content is present in the outer regions of the mantle olivine (Ol. Mantle B.: 2.32 wt%, Table 2), which is also richer in Al_2O_3 than the olivine laths. Small subhedral Ca-rich pyroxene crystals (white arrows in Figs. 5a and 5c, Table 2) are also present.

3.1.6. Chondrule DAG055 BO-1

This chondrule is a *Classic Type* BO chondrule (Fig. 6a) (PTS DAG055, NHM, Vienna). Its parallel thin plates of olivines are set into a glassy mesostasis containing thin pyroxene needles (Fig. 6b). The chondrule is surrounded by a thin olivine crust and rounded to subrounded former metal-rich inclusions, now altered to Fe oxides. Attach to this chondrule is an appendix (lower right corner of Fig. 6a) with barred olivine texture and euhedral to subhedral pyroxenes surrounding the olivine crystals (Fig. 6c). Note that some olivine crystals have lobate surfaces where in contact with the pyroxene (Fig. 6c). The appendix's mesostasis is of clear glass. Voids are common in the matrix and occasionally replace larger portions of it.

There is no chemical variation in the composition of the chondrule and appendix mesostasis. Both are Si–Al–Ca-rich (Ch.M1, Ch.M2, Ap.M., Table 1). Olivine laths in the chondrule have variable FeO contents. Two scan profiles, a ten-step scan

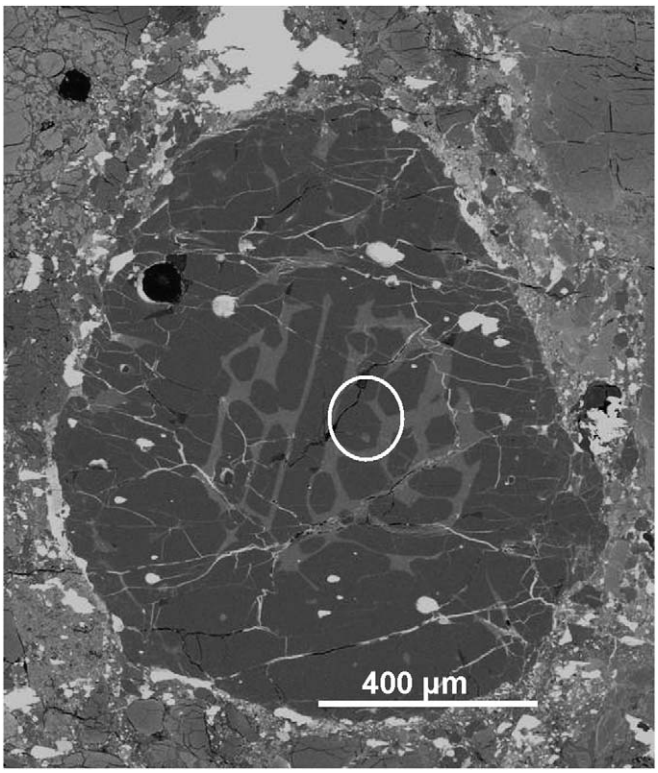

(a)

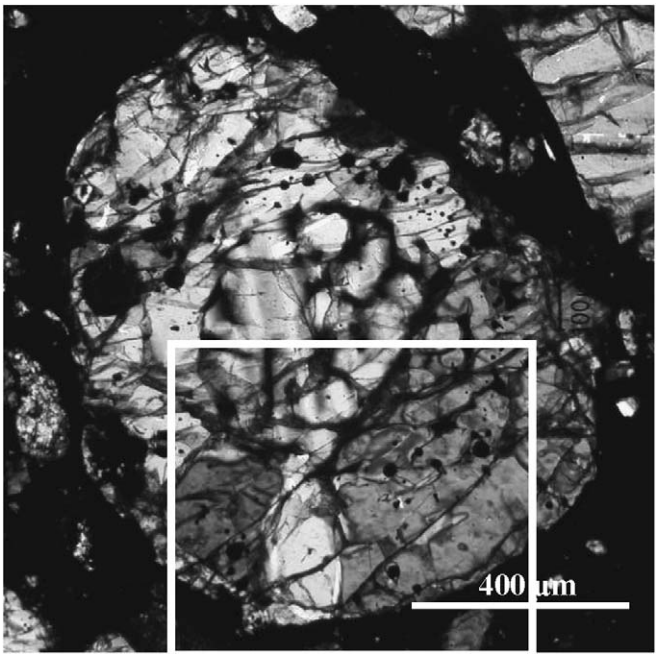

(b)

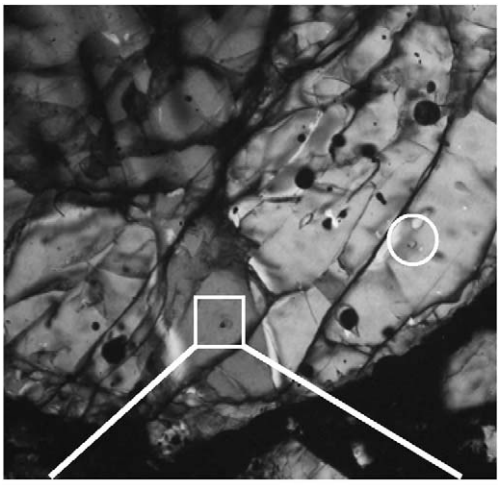

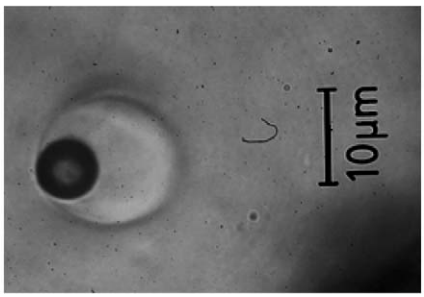

(c)

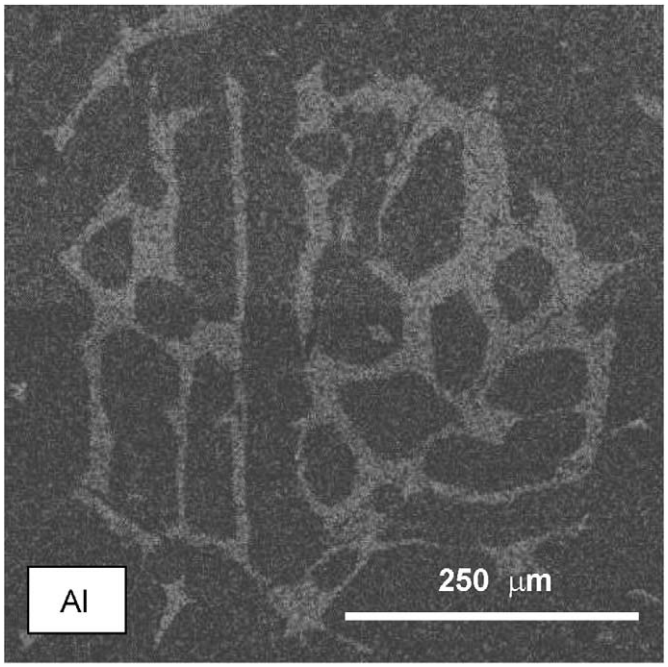

(d)

Fig. 3. (a) BSE image of the Bishunpur-CH-A chondrule (PTS Bishunpur v. G3684). Encircled is the neck inclusion of the core. (b) Transmitted light image showing the core and part of the thick mantle olivines. Note the two optical orientations of the olivines. (c) Transmitted light image of selected region [rectangle in part (b)], showing the location of two primary glass inclusions and an inset with an enlargement of one inclusion. (d–e) SEM Al and Ca images showing the Al–Ca-rich composition of the glassy mesostasis and the neck inclusion from the core.

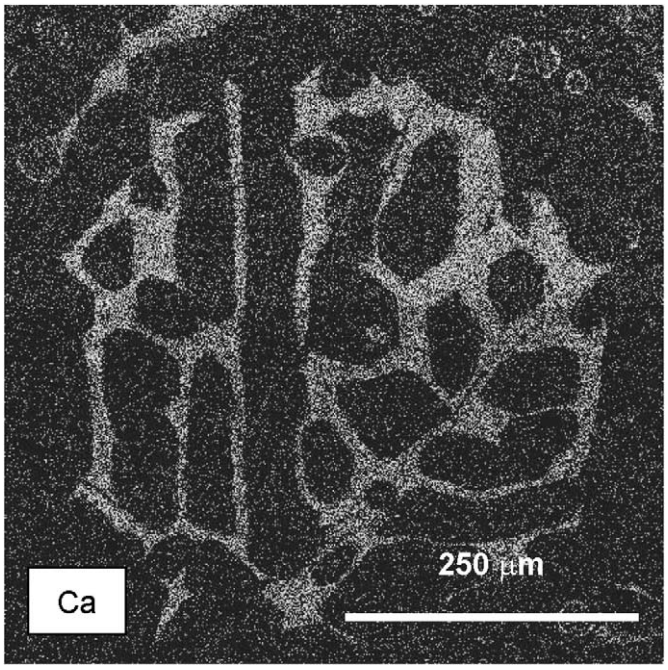

(e)

Fig. 3. (*continued*)

in a high-Fe olivine lath [Ol. Lath (10), Table 2] and a six-step scan in a low-Fe olivine lath [Ol. Lath (6), Table 2] show variations in their FeO contents from 14 to 21.8 wt% and from 3.2 to 5.65 wt%, respectively. Pyroxenes have also variable compositions. The needle-like pyroxenes in the chondrule mesostasis (Ch. Px., Table 2) are high-Ca (20 wt% CaO) and those in the appendix are low-Ca pyroxenes [6.95 wt% CaO: in a five-step scan profile in an euhedral pyroxene in the appendix, Fig. 6c, Ap. Px. (5), Table 2].

3.1.7. Chemical compositions of glasses

Glass inclusions in all studied objects have CaO and Al_2O_3 contents that scatter around the chondritic ratio line (Fig. 7). Those from the mesostasis show super-chondritic (Essebi and Bishunpur Ch-C) and subchondritic (Acfer BO-214/3 and 214/4) CaO/Al_2O_3 ratios, respectively (Fig. 7).

The CaO and Na_2O contents of glass inclusions and mesostasis are anticorrelated (Fig. 8). Inclusion glasses have the highest CaO contents of all glasses and are free of Na_2O.

Trace element abundances in mesostasis glass of Ess-BO-1 are high and typical at 10–20 × CI levels with the exception of Be (100 × CI). Those in Ac-BO 214/3 have high refractory and light rare earth element (LREE) abundances (10 × CI), but lower abundances of Ti (3 × CI), Sc (5 × CI), Ca (4 × CI) and heavy rare earth elements (HREE) (6 × CI) as compare to Ess-BO-1 (Table 3, Fig. 9). Pyroxene (Py Acfer 214/3) in contact with the mesostasis has LREE abundances around 0.5 × CI and HREE abundances around 0.8 × CI, with Ti and Sc abundances similar to those of the mesostasis glass. Trace element abundances in the glass inclusion [Bish Ch-A (GI)] in the Bishunpur chondrule A are higher (∼20–30 × CI) than those in the mesostasis at 10–20 × CI [Bish CH-A(M1-M2), Fig. 10]. All glasses show a similar pattern, that is, unfractionated and high (10–30 × CI) refractory lithophile trace element abundances and low abundances of volatile and moderately volatile elements.

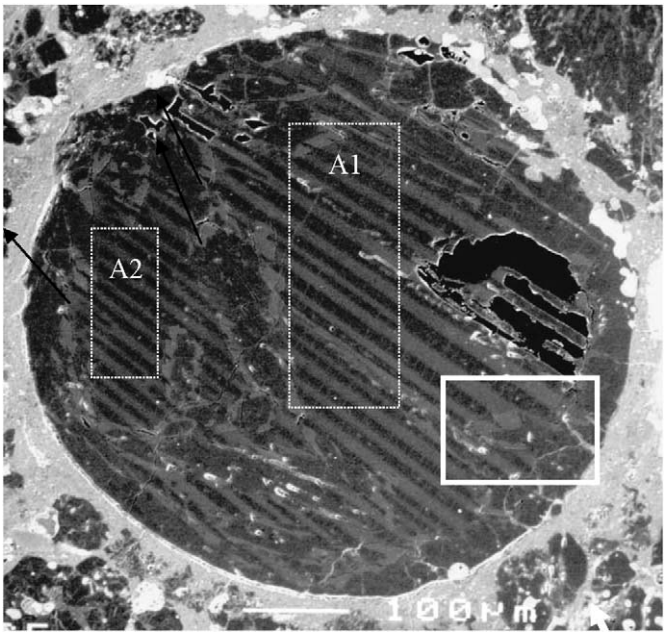

(a)

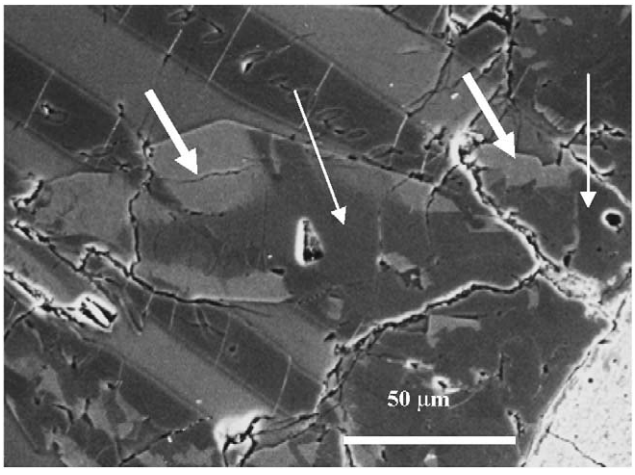

(b)

Fig. 4. (a) BSE image of the AC-BO-214/3 chondrule (PTS Acfer 214 Algerien). Rectangular areas A1–A2 are the selected areas for point counting, as explained in the text. (b) Detail BSE image of the area indicated in part (a), showing the pyroxene with crystal faces against the glass. Arrows (thick and thin) indicates high and low-Ca pyroxene, respectively. (c) SEM Al image of part (b), which clearly shows how the surface of the olivine lath close to the pyroxene is retracting toward the center of the original plate. Arrow indicates glass inclusions in the form of a straight line in the center of the olivine plate. (d) SEM Mg image of part (b), where the wedge of the olivine, where overgrown by the pyroxene, is clearly observed. (e) SEM Ca image of part (b), showing the Ca-rich border of the pyroxene.

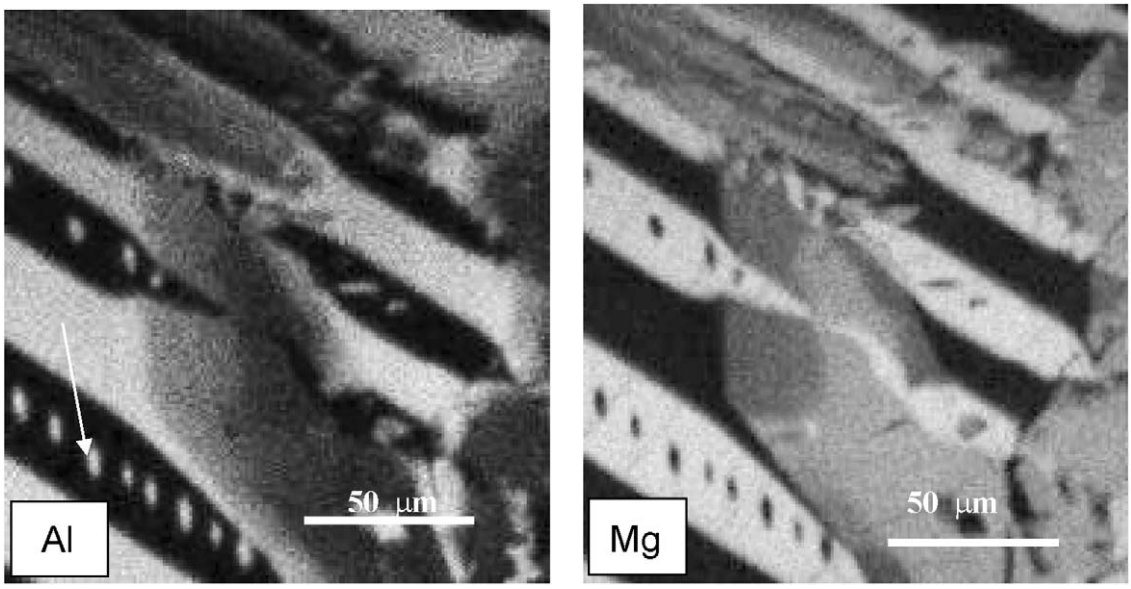

(c) (d)

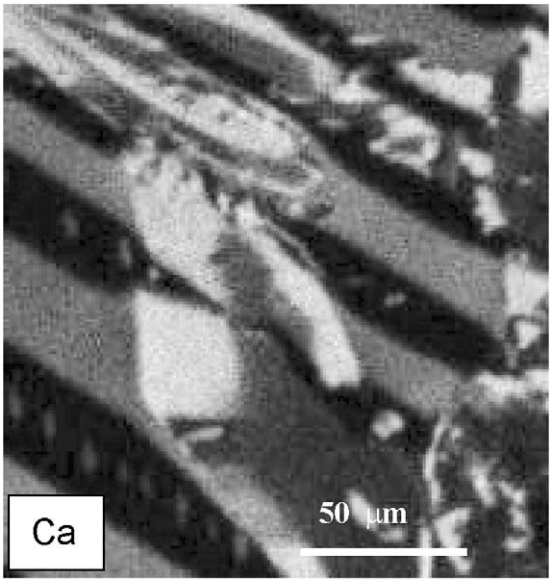

(e)

Fig. 4. (*continued*)

3.2. Bulk compositions of barred olivine chondrules

Bulk compositions were determined for Essebi, Bishunpur A, C and Acfer 214/3 chondrules by point counting. We used a grid to cover the area of the whole object or of selected parts of the chondrule, as explained below.

3.2.1. Ess-BO-1

In this object we covered half of the chondrule area with 3408 points, of which 2284 are on olivine. This gives modal abundances for the constituent phases of: olivine 67%, glass 33%. For the olivine composition we took the mean of the 13 olivine laths given in Table 2. For the glass composition we used the mean value of all glasses (glass inclusions, navel-inclusion and mesostasis, Table 1). The bulk Ess-BO-1 chondrule composition (Table 4) calculated in this way for the four main oxides is: MgO: 39.4 wt%, Al_2O_3: 7.6 wt%, SiO_2: 46.8 wt%, CaO: 6.3 wt%.

3.2.2. Ac-BO-214/3

In this object we selected two areas (A1 and A2, Fig. 4), involving a total of 1050 points. The percentage of the constituent phases in areas A1 and A2 are olivine 63%–glass 37% and olivine 64%–glass 36%, respectively. As for the glass phase composition we used the mean value of all mesostasis glass analyses (Table 1). The olivine composition was calculated from the mean values of Ol. Lath C. (5) and Ol. Lath B. (Table 2). The bulk Acfer 214/3 chondrule composition (Table 4) has 4.33 wt% Na_2O. Because the incorporation of alkalis in the glass is due to a secondary process (as it will be explain in the

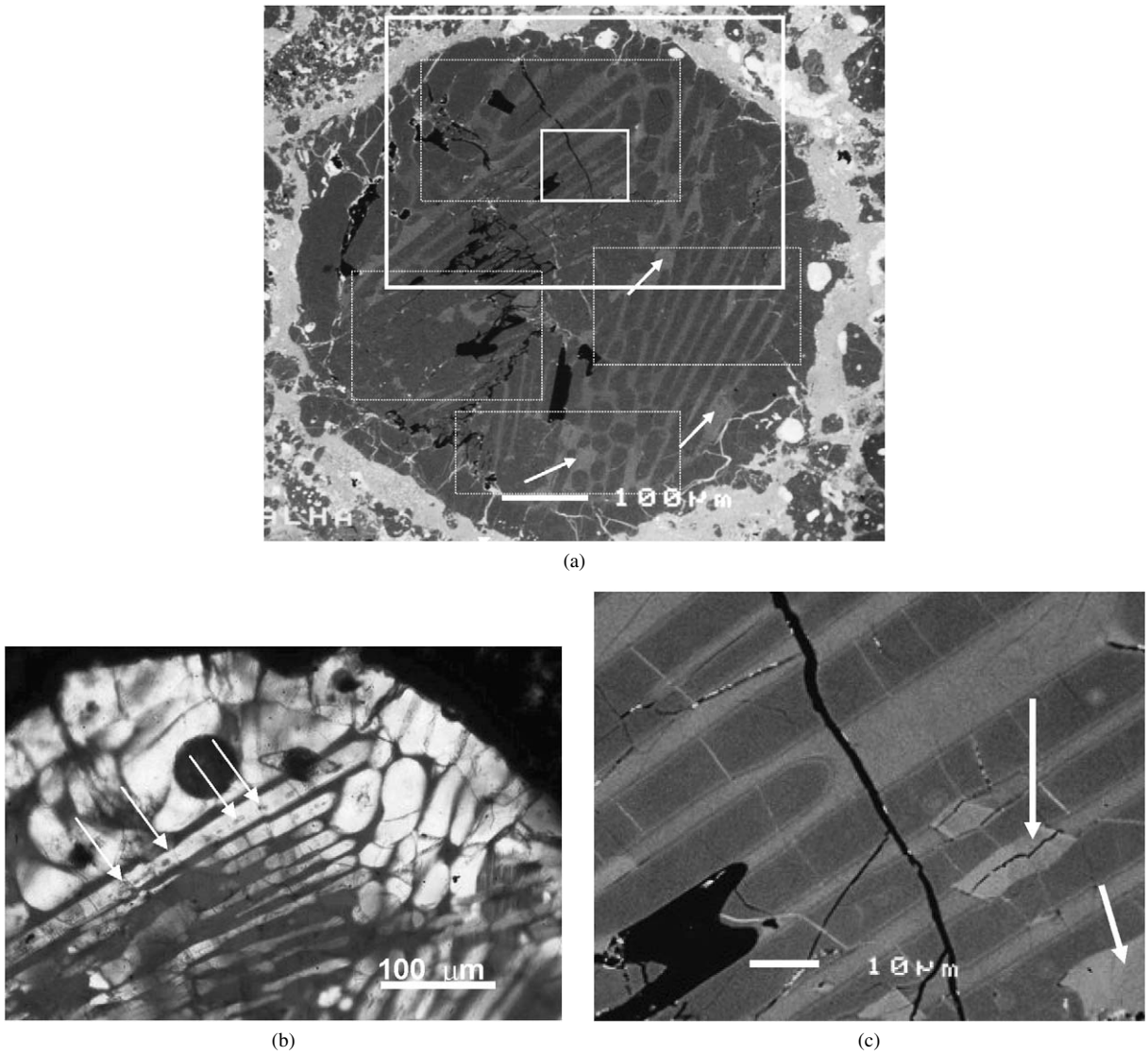

(a) (b) (c)

Fig. 5. (a) BSE image of the Ac-BO 214/4 chondrule (PTS Acfer 214 Algerien), the four rectangular areas (discontinuous thin white lines) are the areas selected for point counting. Arrows show the location of the small pyroxenes. (b) Detail transmitted light image of the area indicated by the big rectangular in part (a). (c) Detail BSE image of the small rectangular area in part (a). Arrows indicate pyroxenes.

text) we have added the content of Na_2O moles to that of CaO to obtain the primary composition. The thus calculated composition, expressed with the four main oxides, is as follows: MgO: 38.2 wt%, Al_2O_3: 7.3 wt%, SiO_2: 47.7 wt%, CaO: 6.8 wt%.

3.2.3. Ac-BO-214/4

In this object we have selected four areas (thin lines in Fig. 5) involving a total of 9500 points from which 2900 were found to be on glass. The modal abundances of these areas is: olivine 70%, glass 30%. For calculating the olivine and glass component of the bulk chondrule we used the mean of all olivines (Table 2). Since the glass inclusions and the mesostasis are all Na_2O-rich, we used for the glass component the mean of all glasses (Table 1). As for the previous chondrule, we added the Na_2O mole content to that of CaO and obtain for the four main oxides: MgO: 40 wt%, Al_2O_3: 6.7 wt%, SiO_2: 47 wt%, CaO: 6.2 wt%.

3.2.4. Bishunpur-A

For estimating the initial composition of this chondrule we selected the barred olivine core area (Fig. 3). From a total of 4240 points, 2560 were on olivine, yielding the abundances: olivine 60%, glass 40%. As glass composition we used that of the glass inclusion (G.I., Table 1). For the olivine composition we took the mean of all olivine crystals from the core (Table 4). The bulk chondrule composition (Table 4) is: MgO: 36.3 wt%, Al_2O_3: 11.5 wt%, SiO_2: 43.7 wt%, CaO: 8.6 wt%.

3.2.5. Bishunpur-C

The area covered by point counting was the whole object (Fig. 2). From a total of 10,265 points, 2267 belong to the glass phase, giving: olivine 78%, glass 22%. Counting in the BO core only gives 5325 points of which 3058 were on olivine, giving a abundances of olivine 57.4% and glass 42.6%.

For the glass and olivine compositions we took that of the glass inclusion (G.I., Table 1) and the mean of all olivines [Ol.

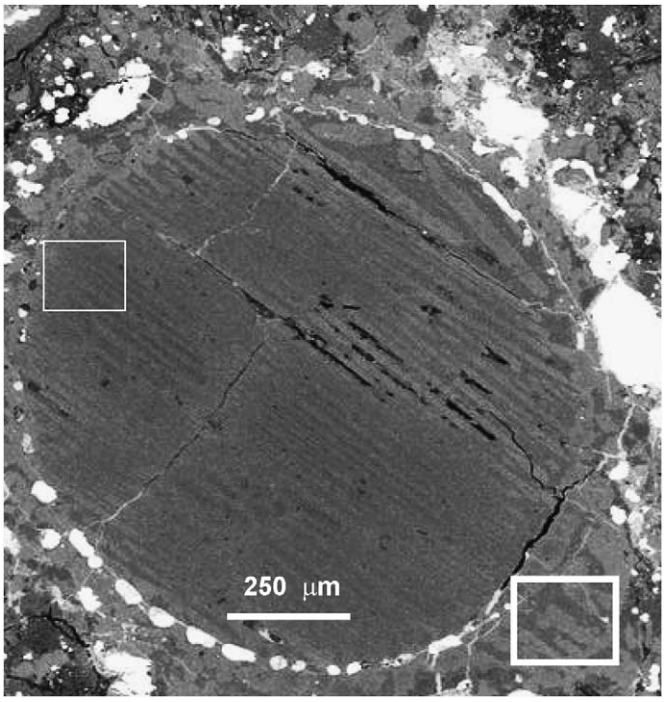

(a)

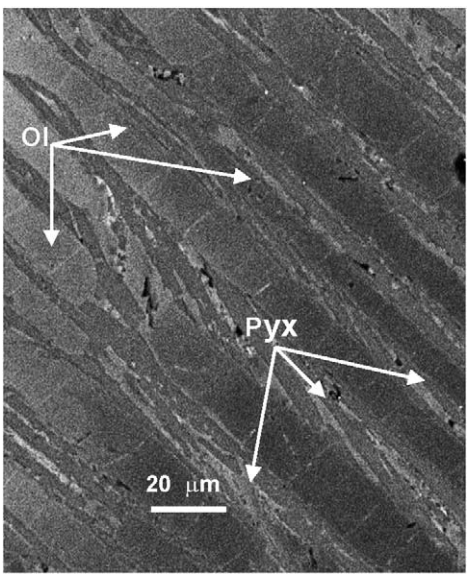

(b)

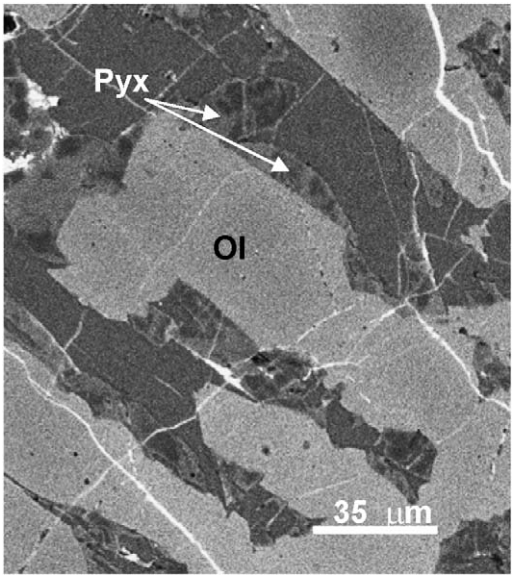

(c)

Fig. 6. (a) BSE image of chondrule DAG055 (PTS DAG 055). (b) Detail BSE image showing olivine laths and needle-like pyroxenes. (c) Detail of the appendix of the DAG055 chondrule [rectangle in part (a)], showing the lobate surface of some olivine crystals in contact with pyroxenes, and the euhedral to subhedral shape of pyroxenes.

H(GI), Ol. Lath (4), Ol. Mantle (4), Table 2], respectively. The olivine from the border (Ol. Mantle B.) was excluded because of its high FeO content.

The BO core composition (Table 4) obtained in this way is: MgO: 40.1 wt%, Al_2O_3: 7 wt%, SiO_2: 46.4 wt%, CaO: 6.5 wt%.

4. Discussion

The formation mechanism for BO chondrules is a topic of ongoing debates. However, there is one point on which almost all researchers agree—in particular for the Classic Barred Type—which is, that such chondrules must have formed from liquid droplets that were undercooled and crystallized rapidly from only one nucleus (e.g., Tsuchiyama et al., 1980; Weisberg, 1987; Hewins, 1988; Lofgren, 1989). Nevertheless, questions remain open about how this liquid could have formed and how the overheating—necessary for destruction of all crystal nuclei—was achieved.

The most popular model has liquid droplets form by melting of solid precursors. The precursors were identified from

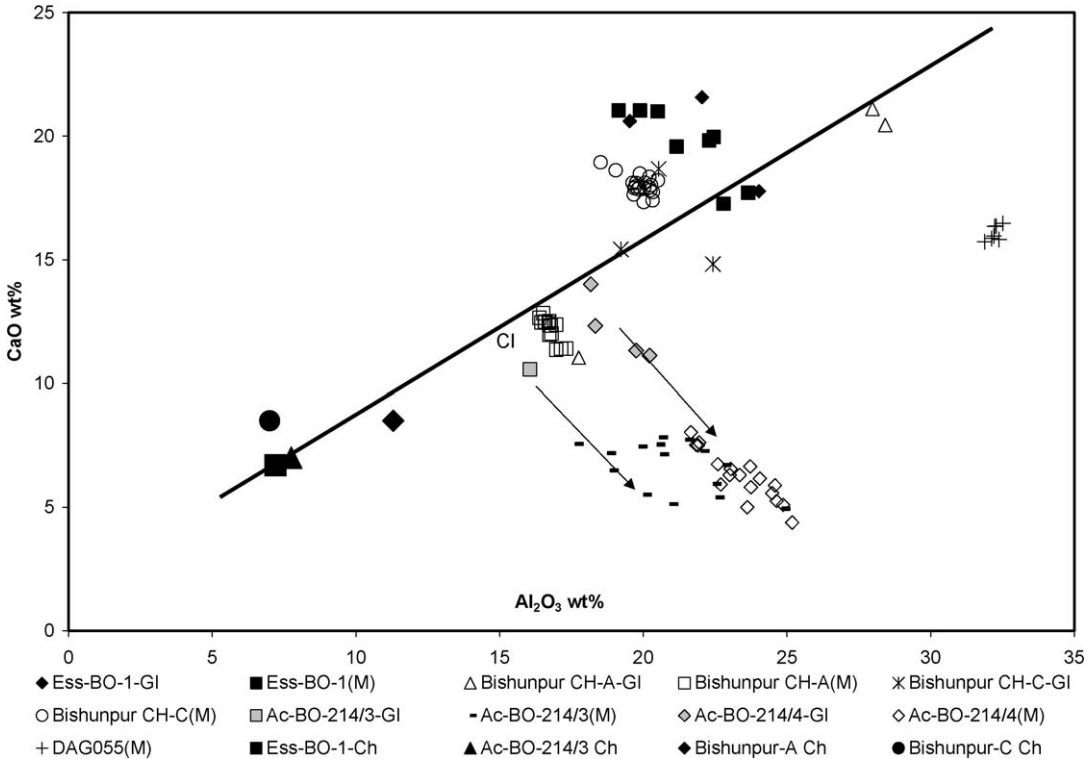

Fig. 7. CaO vs Al_2O_3 diagram of all types of glasses encountered in BO chondrules. Glass inclusions have a chondritic CaO/Al_2O_3 ratio. Note the Ca-depletion in the glassy mesostasis of Ac-BO-214/3 and -214/4.

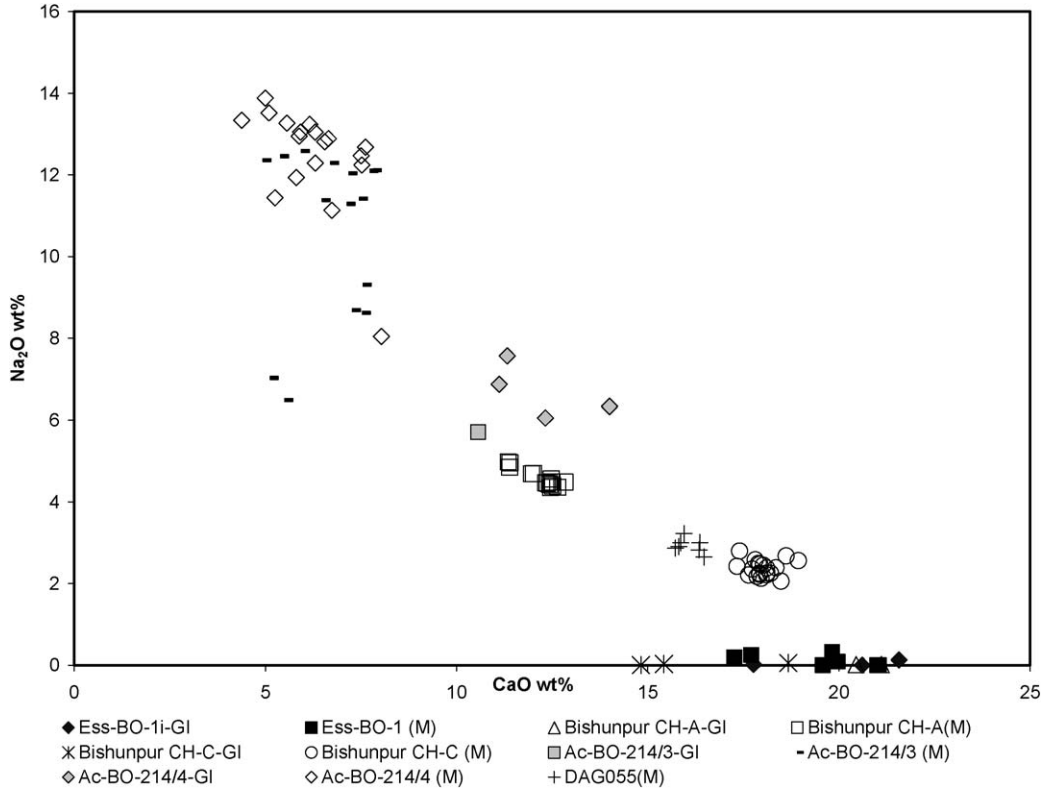

Fig. 8. Na_2O vs CaO diagram of all types of glasses in BO chondrules. Note the lack of Na_2O in the glass inclusions and the glassy mesostasis of Ess-BO-1.

chondrule bulk analyses to consist mainly of two components: a refractory and olivine-rich one and a non-refractory and SiO_2- and FeO-rich one (Grossman and Wasson, 1982, 1983a, 1983b). For Al-rich BO chondrules, a precursor consisting of

Table 3
Ion microprobe analyses (in ppm) of glassy mesostasis in Essebi and Acfer 214 barred olivine chondrules

Element	Ess-BO-1	*Error*	Ac-BO-214/3	*Error*	Ac-BO-214/3	*Error*	Bish Ch-A	*Error*	Bish Ch-A	*Error*	Bish Ch-A	*Error*
			(M1)		(M2)		(Gl)		(M1)		(M2)	
Li	12.9	*0.2*	1.4	*0.06*	0.8	*0.07*	0.84	*0.07*	0.16	*0.009*	0.4	*0.03*
Be	2.19	*0.09*	0.25	*0.02*	0.34	*0.03*	0.43	*0.05*	0.3		0.23	*0.02*
B	0.08	*0.01*	0.28	*0.04*	0.6	*0.09*			0.17	*0.04*	0.4	*0.1*
Sc	42.4	*0.6*	18.7	*0.4*	20	*0.7*						
Ti	4690	*30*	1315	*5*	1420	*9*	6910	*94*	4290	*23*	4430	*42*
V	33.4	*0.7*	46	*0.7*	34.3	*0.9*	57	*1*	37.2	*0.3*	106	*0.9*
Cr	1900	*20*	2570	*7*	1750	*9*	1970	*8*	3230	*3*	3820	*6*
Mn	153	*2*	500	*3*	324	*4*						
Fe	2630	*30*	15,400	*100*	16,000	*190*						
Co	6.4	*0.4*	6.4	*0.4*	12.5	*1*						
Rb	0.24	*0.03*	16.6	*0.8*	21	*2*			0.37	*0.06*	0.3	*0.09*
Sr	70	*1*	36.6	*0.6*	50	*1*	162	*6*	92	*1*	96	*3*
Y	13.2	*0.4*	8	*0.3*	10	*0.5*	26.2	*0.5*	15	*0.1*	15.2	*0.2*
Zr	48	*3*	33.8	*0.9*	41	*2*	79	*1*	39.5	*0.3*	42	*0.6*
Nb	3.6	*0.3*	2.9	*0.2*	2.9	*0.4*	4.6	*0.3*	3.12	*0.09*	3.6	*0.2*
Ba	16.8	*0.8*	8.5	*0.5*	12	*0.9*	58	*1*	28	*0.3*	30	*0.5*
La	2.3	*0.2*	2.3	*0.2*	2.8	*0.3*	5.3	*0.3*	2.54	*0.07*	2.6	*0.1*
Ce	5.5	*0.3*	6.4	*0.3*	6.2	*0.5*	13.3	*0.6*	6.8	*0.1*	7.5	*0.2*
Pr	0.83	*0.07*	0.93	*0.09*	0.9	*0.1*	1.9	*0.2*	1.12	*0.05*	1.4	*0.1*
Nd	4.2	*0.2*	3.8	*0.2*	5.3	*0.3*	10	*0.5*	5.5	*0.1*	6.3	*0.2*
Sm	1.4	*0.1*	1.1	*0.1*	1.2	*0.2*	3.3	*0.4*	1.74	*0.09*	1.9	*0.2*
Eu	0.43	*0.04*	0.32	*0.02*	0.5	*0.05*	1.1	*0.2*	0.75	*0.04*	0.9	*0.09*
Gd	2.2	*0.2*	1.4	*0.1*	0.9	*0.3*	5.9	*0.7*	2.5	*0.2*	3.9	*0.4*
Tb	0.36	*0.05*	0.28	*0.03*	0.18	*0.05*	0.7	*0.2*	0.4	*0.04*	0.46	*0.07*
Dy	2.5	*0.1*	1.5	*0.09*	1.6	*0.2*	6.4	*0.4*	2.9	*0.09*	3.9	*0.2*
Ho	0.48	*0.05*	0.3	*0.02*	0.33	*0.05*	1.2	*0.2*	0.6	*0.04*	0.82	*0.08*
Er	2	*0.1*	0.93	*0.06*	1.2	*0.1*	3.5	*0.3*	1.74	*0.07*	2.6	*0.2*
Tm	0.26	*0.03*	0.15	*0.01*	0.18	*0.04*	0.6	*0.1*	0.25	*0.03*	4.2	*0.06*
Yb	1.68	*0.09*	0.87	*0.08*	0.8	*0.2*	2.8	*0.3*	1.87	*0.08*	2.4	*0.2*
Lu	0.32	*0.04*	0.16	*0.02*	0.2	*0.04*	0.4	*0.1*	0.3	*0.03*	0.4	*0.08*

highly refractory and alkalic materials has also been proposed (Bischoff and Keil, 1984). For these chondrules, impact melting and distillation of equilibrated OC material has been proposed in addition (Krot and Rubin, 1993).

An alternative model, the primary solid condensation model (Kurat, 1988), creates BO chondrules by condensation of fluffy olivine plates from the solar nebula. The large or small stacks of olivine platelets, badly crystallized and highly anisotropic in shape are identified as probably being primitive crystals that can be expected to grow, without the help of a liquid, directly from the vapor phase. The pore space of these vapor-grown crystals will subsequently be partly filled when compounds of volatile elements condense. Finally, a high-temperature annealing event recrystallized the olivine into solid plates and partial melt filled the interstitial space, was chilled and converted to glass.

Based on the present work and on recent observations (Kurat et al., 2004; Varela et al., 2002, 2003), we discuss a third model that allows the formation of BO chondrules directly from the solar nebula by primary liquid condensation without the need for a re-heating event.

In the following paragraphs we will briefly present the basis of this new model to inform the reader about the mechanisms involved. Subsequently, and based on the petrographic and chemical data of each chondrule, we will focus our discussion on their genesis. In doing so, we will confront two models: the melting of solid precursors and the primary liquid condensation models.

4.1. The primary liquid condensation model

The primary liquid condensation model is based on the ability of dust-enriched solar nebular gas to directly condense into a liquid (e.g., Herndon and Suess, 1977; Ebel and Grossman, 2000). Thus, what distinguishes this model from all previous ones is that it does not need a secondary heat source. One heating event is required by all models for the evaporation of presolar dust (e.g., Suess, 1949; Wood, 1962; Blander and Katz, 1967). The melting of solid precursors and the primary solid condensation models need a second heating event for—at least partial—melting of the chondrule precursors. In the 1960s liquids were not recognized to be stable under nebular conditions. That belief made a secondary heating event for the production of liquid droplets necessary. However, Yoneda and Grossman (1995), Ebel and Grossman (2000), and Alexander (2004) have shown that liquids can indeed condense from a solar nebula gas provided the gas/dust ratio is sufficiently low (e.g., Herndon and Suess, 1977). The liquid condensate is expected to have a refractory Ca–Mg–Al-silicate (CMAS) composition (Ebel and Grossman, 2000; Alexander, 2004).

Because liquids can nucleate from a vapor much more easily than crystals, the primary liquid condensation model pro-

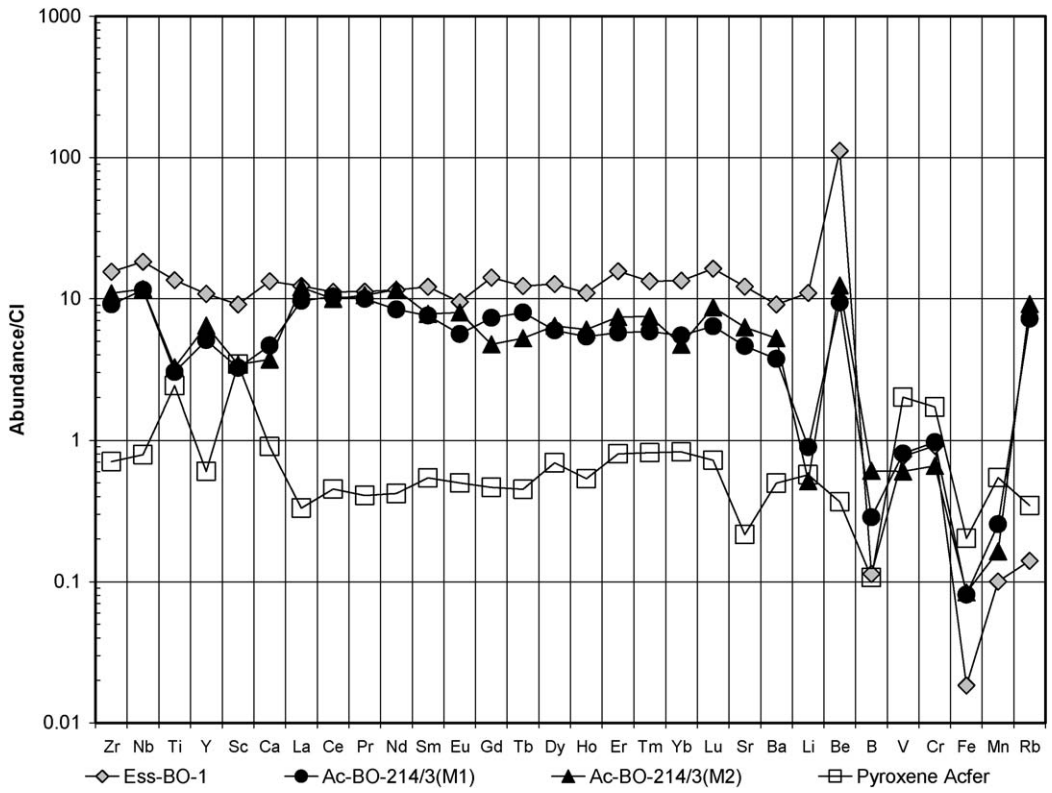

Fig. 9. CI-normalized trace element abundances of the glassy mesostasis of Ess-BO-1 and Ac-BO-214/3 and of the pyroxene in Acfer 214/4. Elements in the trace element abundance plots are arranged in order of increasing volatility, except for the REE, which are arranged in order of increasing atomic number. CI abundances used here and in the following graph are from Lodders and Fegley (2003).

poses that the first condensate to appear in the solar nebula is a liquid. Liquids generated in this way will have a chemical composition that is governed by gas–liquid equilibria. Our studies of different types of glasses in meteorites (CC, OC, EC and achondrites; e.g., Varela et al., 2002, 2003; Varela and Kurat, 2004) showed that liquids (the glass precursors) must have been omnipresent in the solar nebula. They apparently played an important role by facilitating condensation of the major minerals from the solar nebula gas (Kurat et al., 1997; Varela et al., 2005a). This liquid is predicted to be rich in refractory elements and olivine. Thus, once a stable CMAS liquid nucleus is formed and grows into a droplet, an olivine crystal can nucleate in the liquid (see Fig. 8 of Varela et al., 2005a).

Two possibilities can be envisaged:

(1) If the quantity of liquid is low the crystal nucleus will continue growth only where it is covered by the liquid that forms a thin interface between the growing crystal and the vapor. The result will be a grain of irregular shape. The growing crystal will take from the liquid only those elements that will fit into the crystal structure (e.g., Si, Mg, and O), all other elements (usually called incompatible elements) are thereby left in the liquid. The main function of this liquid is to accommodate condensing species, feed the growing crystal with the necessary elements and help to accommodate ions at the proper lattice position of the growing crystal. The incompatible elements such as Ca, Al, and REE, that do not enter the structure of the olivine, will be concentrated in the liquid. Their concentration will be determined by a condensation–evaporation equilibrium between the liquid and the vapor. The crystal will continue to grow epitaxially from the vapor, supported by a thin liquid layer—similar to the vapor–liquid–solid growth process (see, e.g., Givargizov, 1987; Kurat et al., 1997; Varela et al., 2002) or liquid-phase epitaxy. This liquid layer will be preserved by the temperature profile established as an equilibrium between the heat of condensation (liberated at the solid–liquid interface), heat of crystallization and simultaneous heating by impinging gas species that keep the surface relatively hot compared to the inside of the object which is cooled by black-body radiation.
The final product could be a single olivine crystal, or if aggregation of growing crystals took place, an olivine aggregate. With a proper liquid/crystal ratio even a droplet chondrule with porphyritic olivine texture could form (see Varela et al., 2005a).

(2) If the early condensing liquid does not produce a crystal nucleus (homogeneously or heterogeneously) it will continue to grow and will form a sizable (e.g., 200 to 2000 μm) droplet. Eventually a trapped dust grain in the liquid droplet will serve as a crystal nucleus, promoting heterogeneous nucleation. Homogeneous nucleation of an olivine crystal at this stage will need a high degree of undercooling. Growth of that crystal will take place almost simultaneously with nucleation and a plate dendrite (or several, depending on the number of crystal nuclei) will form. As the

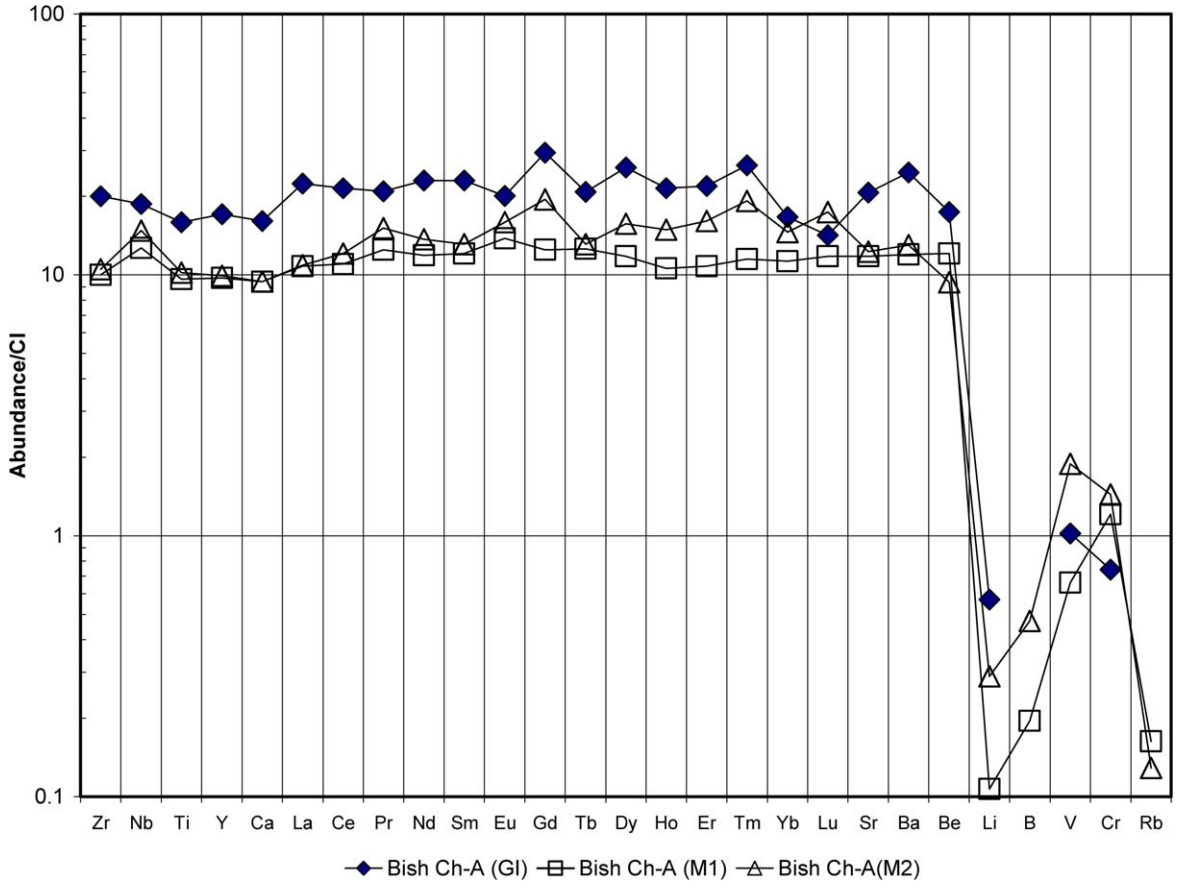

Fig. 10. CI-normalized trace element abundances of the glass inclusion and glassy mesostasis of the Bishunpur Ch-A chondrule.

primary liquid condensation model applies for both the formation of a single crystal and of dendritic plates, the mechanism by which the olivine plates grow is the same as in the previous case. That is, the plates will incorporate only those elements that will fit into the crystal structure while the incompatible elements are concentrated in the liquid. Thus, the residual liquid (the mesostasis glass precursor) will be rich in refractory incompatible elements (e.g., Ca, Al, and REE) and will try to stay in condensation–evaporation equilibrium with the vapor.

4.2. Possible mechanism of formation of barred olivine chondrules

In this section we will discuss the possible origin of BO chondrules based, mainly, on the petrographic features of these objects and add a brief comment about their chemical composition, which will be discussed in more detail later on.

4.2.1. Standard formation model for classic type BO chondrules

Here we discuss the possible mechanisms involved in the formation of the classic barred olivine chondrules like those present in Essebi (C2), Dar al Gani (C3), and Acfer 214 (CH3) chondrites.

One possible way to form classic type BO chondrules is given by the melting of solid precursor model. In this model, the melting temperature must be high and overheating is needed in order to eliminate all crystal nuclei (e.g., Lofgren and Russel, 1985; Radomsky and Hewins, 1987). Dynamic melting and crystallization experiments show that BO chondrules formed after heating to, or somewhat above, their equilibrium liquidus temperature (e.g., Hewins, 1988). The range in this temperature (assuming no seeding) is 1400–1750 °C, with 1500–1550 °C for most cases (Radomsky and Hewins, 1990; Lofgren and Lanier, 1990). The dynamic crystallization studies of BO chondrules by Lofgren and Lanier (1990) show that: "To obtain the BO texture, (1) the preexisting crystalline material, which is presumably an olivine-rich dust, must reach temperatures high enough to cause complete melting: however, (2) the melting must not be so complete as to eliminate all embryos. Melts from which plate dendrites crystallized must have only subcritical embryos. With only subcritical embryos present, a sufficient degree of supercooling can develop before nucleation to stabilized the range of crystals forms characteristic of BO textures." Reaching the above melting conditions is, however, difficult. None of the dynamic crystallization experiments was able to produce a true analogue of the classic single-plate dendrite BO chondrule (Lofgren and Lanier, 1990; Tsuchiyama et al., 1980, 2004).

Another aspect to be considered is the effect of the grain size of the precursor material. Short-duration melting experiments coupled with linear cooling rates (Connolly et al., 1998) show that BO textures can be formed at temperatures around

Table 4
Estimated bulk composition of chondrules Ess-BO-1, Acfer 214/3 and Acfer 214/4

	Ess-BO-1				
	Glass	Glass Perc. 33	Olivine	Oliv. Perc. 37	Ch. Bulk
SiO_2	53.7	17.7	42.2	28.3	46.0
TiO_2	1.05	0.34	0.08	0.05	0.40
Al_2O_3	22.3	7.4	0.17	0.11	7.5
Cr_2O_3	0.35	0.12	0.29	0.19	0.31
FeO	0.23	0.08	0.80	0.54	0.61
MnO	0.04	0.01	0.04	0.03	0.04
MgO	3.92	1.29	55.9	37.5	38.7
CaO	18.3	6.0	0.30	0.20	6.2
Na_2O	0.16	0.05			
K_2O					
Total	99.96	32.99	99.78	66.85	99.82
	Acfer 214/3				
	Glass	Glass Perc. 33.5	Olivine	Oliv. Perc. 63.5	Ch. Bulk
SiO_2	55.1	20.1	41.9	26.7	46.8
TiO_2	0.60	0.22	0.05	0.03	0.25
Al_2O_3	19.3	7.03	0.22	0.14	7.2
Cr_2O_3	0.35	0.13	0.14	0.09	0.2
FeO	1.27	0.46	0.88	0.56	1.0
MnO	0.05	0.02	0.14	0.09	0.1
MgO	4.55	1.66	56.3	35.8	37.5
CaO	7.6	2.79	0.22	0.14	2.93
Na_2O	10.3	3.76			3.76
K_2O	0.85	0.31			0.31
Total	99.96	36.49	99.84	63.50	99.99
	Acfer 214/4				
	Glass	Glass Perc. 30.0	Olivine	Oliv. Perc. 70.0	Ch. Bulk
SiO_2	52.6	15.8	42.9	30.0	45.8
TiO_2	0.40	0.12	0.00	0.02	0.14
Al_2O_3	21.3	6.40	0.2	0.11	6.5
Cr_2O_3	0.45	0.14	0.40	0.27	0.4
FeO	1.72	0.52	1.60	1.11	1.6
MnO	0.03	0.01	0.10	0.06	0.1
MgO	2.82	0.85	54.6	38.2	39.1
CaO	8.8	2.65	0.2	0.17	2.82
Na_2O	10.7	3.21	0.00	0.01	3.22
K_2O	1.11	0.33			0.33
Total	99.95	30.03	100.00	69.95	99.98

Table 4 (*continued*) Estimated bulk composition of chondrules Bishunpur-A, Bishunpur-C and CIPW norms of all studied objects

	Bishunpur-A					
	Glass	Glass Perc. 40	Olivine	Oliv. Perc. 60	Core Bulk	Ch. Bulk Oliv:88 + GI:12
SiO_2	44.5	17.8	41.9	25.2	43.0	42.2
TiO_2	1.08	0.43	0.02	0.01	0.4	0.15
Al_2O_3	28.2	11.3	0.06	0.04	11.3	3.44
Cr_2O_3	0.26	0.10	0.22	0.13	0.2	0.22
FeO	0.47	0.19	0.85	0.51	0.7	0.81
MnO	0.01	0.00	0.02	0.01	0.0	0.02
MgO	4.27	1.71	56.6	34.0	35.7	50.3
CaO	20.8	8.32	0.23	0.14	8.5	2.69
Na_2O						
K_2O						
Total	99.59	39.84	99.93	59.96	99.79	99.89
	Bishunpur-C					
	Glass	Glass Perc. 22	Olivine	Oliv. Perc. 78	Ch. Bulk	Core Bulk Oliv:57.4 + GI:42.6
SiO_2	53.3	11.7	41.5	32.4	44.1	46.5
TiO_2	0.94	0.21	0.03	0.02	0.23	0.42
Al_2O_3	20.5	4.51	0.14	0.11	4.6	8.8
Cr_2O_3	0.35	0.08	0.21	0.17	0.24	0.27
FeO	0.63	0.14	1.58	1.23	1.37	1.17
MnO	0.02	0.00	0.04	0.03	0.04	0.03
MgO	4.92	1.08	56.2	43.8	44.9	34.3
CaO	18.7	4.11	0.33	0.26	4.37	8.2
Na_2O	0.05	0.01			0.01	0.00
K_2O						
Total	99.41	21.87	100.00	78.00	99.87	99.69

CIPW norm	Ess-BO-1	Acfer 214/3	Acfer 214/4	Bishunpur-A	Bishunpur-C
Plagioclase	19.9	16.3	10.5	9.41	12.4
Orthoclase			1.95		
Nepheline		10.0	10.4		
Diopside		9.2	9.1		7.1
Hypersthene	19.8				6.4
Olivine	51.7	64.0	67.7	89.1	73.7
Larnite				1.23	
Rutile	0.31				
Ilmenite	1.33	0.47	0.27	0.23	0.44
Sphene	7.1				
	100.0	100.0	100.0	100.0	100.0

2100 °C, that is 400 °C above the liquidus, provided the precursor material is coarse-grained. However, obtaining such a precursor material is very difficult, as condensation of solids does not produce large and well-ordered crystals. Grains formed in condensation experiments are very small, varying from 20 to 60 nm in diameter, and can form fluffy and open aggregates consisting of hundreds to thousands of individual grains (e.g., Rietmeijer et al., 2002; Nuth et al., 2002). If the precursor material is fine-grained (similar to nebular condensates), simple rapid heating will produce very fine-grained chondrules, like dark-zoned chondrules (Hewins and Fox, 2004)—and they will have identical chemical composition.

In summary, forming classic type BO chondrules by melting of solid precursors requires taking into consideration several aspects: (1) complete melting plus overheating that will eliminate all nuclei, (2) cooling of the system: homogeneous nucleation will take place only after some undercooling, (3) the first nucleus has to crystallize instantaneously to form one crystal for the whole droplet, giving rise to the BO chondrule. Formation of a multiple-plate dendrite, like that of Acfer 214/4, by melting of solid precursors seems to be easier as evidenced by the success in replicating such textures (e.g., Tsuchiyama et al., 2004), because several nuclei can remain.

Another possible way to form the classic type BO chondrules is described by the primary liquid condensation model. In this model, all aspects concerning the precursor material (e.g., the grain size or the initial precursor melange) as well as all the parameters involve in the melting process (e.g., peak temperatures, heating times, kinetics of melting) need not to be considered. The initial material is already in the liquid state and it has a refractory composition. The condensate liquid will be Ca–Mg–Al–silicate-rich (Ebel and Grossman, 2000;

Alexander, 2004). Once the droplet of CMAS liquid is formed, nucleation and growth can occur simultaneously at a sufficient degree of undercooling, giving rise to a plate dendrite.

Both models appear to allow the formation of the classic type BO chondrules (e.g., Ess-BO-1, Acfer 214/3) and possibly also the discontinuous BO chondrule of Bishunpur C. The main difference is the simplicity provided by the primary liquid condensation process, which produces a liquid droplet condensate from the nebular gas that produces the chondrule in just one step.

4.2.2. Formation of barred olivine chondrules with a thick mantle

The formation of a chondrule like Bishunpur Ch-A apparently takes more steps. First, its shape is not that of a droplet and, second, its bulk composition is extremely olivine-rich, a composition which is not likely to be that of a liquid. On the other hand, the BO core retains the signature of a liquid and a crystallization history similar to that of Ess-BO-1 but with two olivine nuclei. In addition, glass inclusions in the mantle olivine document the presence of a liquid during its formation.

If Bishunpur Ch-A is a crystallized melt droplet formed according to the melting of solid precursor model, mantle olivines are expected to have formed first, after which the core formed from the residual melt during rapid cooling. Because the composition of all olivines in the chondrule (mantle and core) remains uniform and because no pyroxene is present, the composition of all glasses (e.g., primary glass inclusions and the glassy mesostasis of the core) should be also very uniform. However, this is not what is observed. The glasses in the core and in the olivine mantle have different compositions: glass inclusions in olivine have CMAS composition, but the mesostasis glass of the core is alkali-rich. One way to overcome this discrepancy is to suppose that the initial mixtures of solid precursors include some alkali components that give rise to alkali-rich glasses. The glass inclusions in the olivine mantle, initially similar to the mesostasis in their compositions, lost their alkalis in an evaporation process. This process could have affected more intensively those glasses located near the border of the object, while the mesostasis remained alkali-rich. However, this process is unable to explain the difference in the CaO content between the glass inclusions and in the mesostasis.

In addition, the non-spherical shape of Bishunpur Ch-A and its very high olivine content argue against formation from a liquid droplet with the composition of the bulk chondrule. In contrast to the whole chondrule, the core is perfectly round, which cannot be expected if it formed from the residual liquid that produced also the mantle olivines. In addition, the core has a BO texture, indicating an origin from an all-liquid droplet.

This situation forces us to suggest another, simple, formation history for this chondrule: the BO core formed from an undercooled liquid droplet primary condensate by simultaneous crystallization of two nuclei. Once the core had been formed, both crystals forming the BO shell continued to grow epitaxially from the vapor, supported by a thin liquid layer (Varela et al., 2005a). Preferential growth will follow certain (imperfection) directions, will be governed by the availability of liquid, and will lead to a non-spherical shape of the chondrule. The most important function of the thin liquid layer is to help the crystal grow by accommodating condensing species and feeding the growing crystal with the necessary elements. Because the role of this liquid is to serve as support for the growth of whatever phase is oversaturated in the vapor, the trace element contents in the liquid (the glass precursor) will always be high and independent of the crystal it is associated with (Varela et al., 2005a). Therefore, we can expect the chilled liquid (= glasses) to have uniform trace element contents throughout a given chondrule, and this is what we observe in our chondrules as well as in aggregates we previously described (Varela et al., 2005a).

Compositional variations among glasses in Bishunpur Ch-A apparently are the result of a secondary process. The glass inclusions in olivine have chemical compositions that agree with those predicted for liquids of high-temperature solar liquid condensates (e.g., Alexander, 2004; Ebel and Grossman, 2000), i.e., they are rich in Ca and Al and free of alkali elements. In contrast, mesostasis glass of that chondrule is rich in alkalis and poor in Ca. This situation is very common in chondrules and aggregates of primitive chondrites and has been interpreted by us (Kurat and Kracher, 1980; Varela et al., 2002, 2005a) to be the result of a vapor–glass exchange reaction in which Ca in the glass was replaced by Na from the vapor. This process likely also occurred in chondrule Bishunpur Ch-A.

In contrast, the isolated primary glass inclusion in the olivine mantle retained the memory of the original refractory composition of the liquid that helped to grow the olivine. The chemical composition of these glasses, rich in incompatible elements (e.g., Al, Ca) and with unfractionated and high REE contents, but depleted in volatile and moderately volatile elements, signal vapor fractionation and a common origin for both (mesostasis and glass inclusions) glasses.

The olivine shells in the BO chondrules Bishunpur-C and Acfer 214/4 show several surface features (e.g., indentations and lobate surfaces) indicating that their shapes are not that of a liquid droplet. In the case of Bishunpur-C the high percentage of the olivine component (78%) in the total chondrule argues against its formation from a liquid droplet. In addition, its thick olivine rim as well as its surface features suggests that olivine continued to grow after the BO chondrule core had formed. A similar process could have given rise to the irregular mantle olivine observed in Acfer 214/4. Thus, while some objects (e.g., Ess-Bo-1) seem to be the result of the direct condensation of a liquid droplet, others seem to have grown a BO core first, while the shell (olivine rim) continued to grow epitaxially from the vapor, supported by a thin liquid layer.

In summary, the melting of solid precursors model can easily produce a multiplate dendrite chondrule, but is unable to produce objects like the Bishunpur C chondrule. The primary liquid condensation model can explain the formation of all studied objects.

4.3. Chemical compositions of barred olivine chondrules

From a chemical point of view, Ess-BO-1 and Bishunpur A are pristine. Their mesostasis glasses have a nearly chondritic

Ca/Al ratio and are free of any alkali elements (Na, K, and Rb). On the other hand, the mesostasis glass in the Acfer 214/3 chondrule has high contents of alkali elements. However, trace element abundances in Ess-BO-1 and Acfer 214/3 chondrules have a similar pattern (Fig. 9). This pattern, ubiquitous in glasses in chondrites and achondrites (Kurat et al., 1997; Varela et al., 2002, 2003, 2005b), indicates formation by condensation. The high abundances of all refractory elements is due to buffering by the vapor that, at the time of formation of a single perfect or barred olivine crystal, is oversaturated in all refractory elements (e.g., Varela et al., 2005a).

However, Acfer 214/3 has low contents of Ti, Y, Sc, and Ca (∼3 × CI), HREE fractionated with respect to LREE, and a high Rb content. Petrographic evidence shows that in the Acfer 214/3 chondrule pyroxene grew at the expense of olivine. Because trace element contents in glasses show fractionation due to the crystallization of pyroxene, its growth must have taken place at high speed shortly before the liquid was chilled to glass. The glass could not have its trace element content buffered by the vapor because of the slow diffusion rate of the highly charged ions in the liquid. This is similar to what has been observed in some glasses in the angrite D'Orbigny (Varela et al., 2003).

4.3.1. Alkali abundances

If BO chondrules formed by the melting of solid precursors process, the chemical composition of chondrules can be considered to be either a property inherited from their precursors (if chondrules formed as closed systems; e.g., Grossman, 1988), or the result of changes by chemical reactions with the vapor or by fractional evaporation of moderately volatile elements (if chondrules formed as open systems; e.g., Matsuda et al., 1990; Alexander, 1996; Sears et al., 1996). Alkali loss during remelting seems difficult to avoid. The study of alkali abundances in Allende BO chondrules (Matsuda et al., 1990) showed a positive correlation between bulk alkali and olivine Fa contents in these chondrules. To explain these results the authors concluded that, because the olivine Fa content is an indicator of the oxidation state of the system MgO–Fe–SiO_2–O (Nitsan, 1974), BO chondrules with low olivine Fa contents formed from reduced melts. Because the volatilization rate of Na increases with decreasing oxygen partial pressure (Tsuchiyama et al., 1981) and because due to flash heating and rapid cooling the interaction of the condensate with the nebular gas seems to be incomplete Matsuda et al. (1990) concluded: "the volatilization of alkalis was controlled mainly in the conditions produced by melts themselves and thus more intensive volatilization of alkalis may have occurred from the more reduce BO melts, which in turn produced lower olivine Fa." The experiments by Tsuchiyama et al. (2004) to reproduce BO textures suggest that chondrules formed as open systems. They indicate that evaporation of Na and Si can explain the variations of alkali and olivine abundances in chondrules. However, evaporation should produce also isotopic mass fractionation. Experiments show that, indeed, the evaporative loss of K will increase δ^{41}K in the evaporation residue, consistent with Rayleigh fractionation (Yu et al., 1998). However, no fractionation of K and Si isotopes is observed in natural chondrules. Furthermore, oxygen isotope studies of Allende chondrules point toward a gas/melt interaction process (Clayton et al., 1983; Jones et al., 2004) and explain the lack of isotopic mass fractionation (Humayun and Clayton, 1995). In addition, a K isotope study of glass mesostasis and glass inclusions in Bishunpur chondrules (Alexander et al., 2000) clearly showed that no K isotope Rayleigh mass fractionation had taken place. Moreover, K isotope fractionation is absent in the glass inclusions as well as in the mesostasis. Thus, if BO chondrules formed by melting of solid precursors, there is a discrepancy between the experimental results on chondrule formation and the results obtained from natural objects. Because glass inclusions and mesostasis can behave as either closed or open systems, respectively, if K loss occurred during melting, the lack of isotopic mass fractionation can be explained if K exchange with an isotopically normal reservoir took place, either during or after formation of chondrules (Alexander et al., 2000).

Another way to explain the alkali variations in BO chondrules is by applying the primary liquid condensation model. According to this model alkali variation in glasses of mesostasis and glass inclusions can be produce by an exchange reaction between glasses in the chondrule and the cooling nebula (Kurat et al., 2004; Varela et al., 2005a). Once the BO chondrule is formed, temperatures in the nebula will drop, allowing condensation of alkali elements (e.g., Na, K, Rb). The Na_2O vs CaO anti-correlation shown by these glasses (Fig. 8) (similar to that observed for Na-rich glasses in CR and CV3 chondrites; Varela et al., 2002, 2005a) seems to be the result of a glass–vapor exchange reaction that replaced Ca by the volatile elements Na and K. This process, which likely occurred under subsolidus conditions, involves the exchange of fairly mobile network modifier cations (Varela et al., 2005a). In addition, the fact that the anti-correlation is exhibited by glasses that have acted as open systems (e.g., compare the Bishunpur Ch-A and Ch-C and Acfer 214/3 and 214/4 mesostasis and glass inclusions, Fig. 8) suggests that this exchange is a secondary process that had mainly occurred after formation of the glass inclusions. Since according to this model variations in the alkali content of glasses are acquired during cooling, no evidence of isotopic mass fractionations in chondrules is expected—exactly what is observed in natural objects (Alexander et al., 2000).

4.3.2. Silica abundance

In addition to Na enrichments, mesostasis glasses of those chondrules that have behaved as open systems (e.g., Bishunpur Ch-A, Table 2) are also enriched in Si compared to glass inclusions in olivine, similar to what has been observed in chondrules from the Kaba CV3 chondrite (Varela et al., 2005a). It is thus possible that the increase of Si in the liquid of BO chondrules in Ac-BO-214/3, Ac-BO-214/4, and DAG 055 caused a reaction with the olivine to form pyroxenes. The subsolidus exchange of Ca for Na, however, changed the glass composition from originally silica-oversaturated to highly silica-deficient. The new composition is highly nepheline-normative and obviously out of equilibrium with the pyroxene. Because the pyroxene should have reacted back to olivine but we cannot detect

Table 5
Estimation of the chemical composition of the initial liquid drop to form BO chondrules

	Ess-BO-1	Acfer 214/3	Acfer 214/4	Bishunpur-A	Bishunpur-C	Initial drop BO liquid	Mole fraction
SiO_2	46.8	47.7	47.2	43.7	47.5	46.6	40.4
Al_2O_3	7.6	7.5	6.7	11.5	9.0	8.5	4.3
MgO	39.4	38.2	40.2	36.3	35.1	37.8	48.7
CaO	6.3	6.5	5.9	8.6	8.3	7.1	6.6
Total	100.1	99.9	100.0	100.1	99.9	100.0	

any sign of such a reaction, the Ca–Na exchange must have taken place between the vapor and the glassy and not the liquid mesostasis.

4.3.3. Fe abundance

Olivines in all studied chondrules have low contents of FeO. Only in some objects, the FeO content is higher in the mantle olivine. This is clearly observed in Bishunpur-C, where an increase of 5.8 wt% in the FeO content can be observed between the mean of 4 analyses of the olivine shell and an analysis very closed to the chondrule surface (Table 2).

Our bulk chemical compositions for the CM2, LL3.1, CH3, and C3-UNGR BO chondrules are thus less enriched in FeO than those observed in the BO chondrules of ordinary chondrites H3, L3, and LL3 (with FeO contents varying from 13.6 to 16.1 wt%; Weisberg, 1987). The only object from our collection that shows FeO contents similar to those observed by Weisberg (1987) is DAG 055 BO-1 (Table 2). In this object several olivine laths show an increase in Fe content from the core toward the surface of the olivine. In addition, we can observe the existence of areas with Fe-poor olivines and others with Fe-rich ones. The latter occur mainly close to fractures that crosscut the object (Fig. 6) suggesting late metasomatic addition of Fe to the BO chondrule.

In summary, variations in the chemical compositions of chondrules (e.g., alkali and Si contents, Fe/Mg ratio) can be produce when these objects behave as open systems and thus can exchange elements with the cooling vapor. However, those chondrules (e.g., Ess-BO-1 and Bishunpur Ch-C) that behaved as relatively closed systems avoided exchange reactions and as a consequence the composition of the glass inclusions in olivine and the glassy mesostasis remained similar to each other and apparently reflect the pristine chemical composition of the liquid.

4.4. The chemical composition of liquid droplets that formed BO chondrules

In an attempt to find the chemical composition of the initial liquid droplet that could have given rise to BO chondrules we have determined the bulk chemical compositions of the studied BO chondrules. Essebi-BO-1 is a pristine object and its bulk chemical composition (SiO_2: 46.8 wt%, MgO: 39.4 wt%, Al_2O_3: 7.6 wt%, CaO: 6.3 wt%, Fig. 7) can be taken to represent that of the primary condensate liquid. Indeed, its composition agrees with that of the liquid predicted by Ebel and Grossman (2000) and Alexander (2004). In the case of Ac-BO-214/3 and Ac-BO-214/4, because the mesostasis is enriched in alkalis, which in the primary liquid condensation model are acquired in a secondary process, we have added the Na_2O content to that of CaO. If this is done, the chemical compositions of Ac-BO-214/3 (SiO_2: 46.8 wt%, MgO: 37.5 wt%, Al_2O_3: 7.2 wt%, CaO: 6.5 wt%) and Ac-BO-214/4 (SiO_2: 47.05 wt%, MgO: 40 wt%, Al_2O_3: 6.7 wt%, CaO: 5.89 wt%) are very similar to that of Ess-BO-1 (Table 5) and also match the composition expected for a primary condensate liquid. For Bishunpur Ch-A, if we correct for the metasomatic alterations suffered by the glass of the core by adjusting its composition to that of the primary glass inclusions (Si–Al–Ca-rich) of the mantle, we obtain an original chemical composition of the core of: SiO_2: 43.7 wt%, Al_2O_3: 11.5 wt%, MgO: 36.3 wt%, and CaO: 8.6 wt%, comparable to that of Ess-BO-1 (Fig. 7), but slightly more refractory. In the case of Bishunpur-C, the thick olivine rim suggests that olivine continued to grow after the BO chondrule core had formed, as is indicated also by the high abundance of the olivine component (78%) in the total chondrule. Counting the BO core only gives constituent percentages of olivine 57.4% and glass 42.6%. The BO core composition of Bishunpur-C (MgO: 35.1 wt%, Al_2O_3: 9 wt%, SiO_2: 47.5 wt%, CaO: 8.3 wt%) is also in agreement with that of a primary condensate liquid.

Considering the uniformity in the bulk chemical compositions of all studied BO chondrules, we propose the chemical composition of the liquid droplet from which BO chondrules evolved: SiO_2: 46.6 wt%, MgO: 37.8 wt%, Al_2O_3: 8.5 wt%, CaO: 7.1 wt% (Table 5). Based on Alexander's (2004) results, and considering a temperature of 1700 °C and a pressure of 10^{-3} atm, the primary condensate liquid from which BO chondrules could have formed will form in regions of the solar nebula with a CI dust enrichment of ∼700× over the solar composition.

5. Conclusions

Our petrological and geochemical studies of BO chondrules from LL3.1, CM2, CH3, and C3-UNGR chondrites revealed that they likely represent primary liquid condensates of the solar nebula. Their bulk major and trace element composition is compatible with that theoretically predicted for early solar nebula liquid condensates. An origin by direct liquid condensation from the solar nebula considerably simplifies the genesis of these omnipresent chondrules. In this process, refractory, olivine-rich chondrules of fairly uniform chemical composition are produced in just one step. Compositional variation is achieved by continued processing in the cooling nebular gas. The following processes are identified to have played a major role in the formation of BO chondrules:

- Condensation of a $MgO–SiO_2–CaO–Al_2O_3$-rich liquid from the nebular gas, forming chondrule-sized droplets (e.g., 200 to 2000 μm).
- Strong undercooling of the liquid by black-body radiation.
- Homogeneous or heterogeneous nucleation of typically just one olivine crystal.
- Very fast crystallization of that olivine into a multi-plate dendrite.
- Epitaxial growth of olivine at the surface of the mostly crystalline droplet by the vapor–liquid–solid process.
- Fast continued cooling and quenching of the remaining liquid to glass.

After these steps, the primitive BO chondrule is created. It will consist of a BO core of platy olivine and $SiO_2–CaO–Al_2O_3$-rich glass and will be mantled by a crust made of olivine that has the same crystallographic orientation as the olivine plates of the core. Compositionally, the BO cores of such chondrules—like chondrule Ess-BO-1—are very similar to each other, as can be expected for early liquid condensates from the solar nebular gas. Some compositional variation is present among such chondrules because of variations in the acquisition of epitaxially grown olivine. The typical proportions of constituting glass (the carrier of the refractory lithophile elements) and olivine of 37 and 63 vol%, respectively, can be considerably altered in this way.

Continuing communication of such primitive chondrules with the cooling nebula will lead to various elemental exchanges between the chondrule and the nebular gas. That way the chondrule

- will acquire Fe^{2+} (and Cr^{3+}, Mn^{2+}, etc.) for Mg^{2+},
- will acquire Na^+ and K^+ (and other alkalis) for Ca^{2+},
- will acquire Be and B, and
- will exchange ^{16}O for ^{17}O and ^{18}O to isotopically adjust to the abundances in the new nebula region.

Because all of these processes usually do not achieve equilibrium between the solid chondrule and the gas (do not run to completion), many compositional variations can be produced. In that way, each chondrule will acquire its own chemical and isotopic composition. Parent body alterations could create additional mineralogical, chemical and isotopic variety.

This primary liquid condensation model of BO chondrule formation fits into the general formation model of common porphyritically textured chondrules and aggregates by vapor–liquid–solid condensation and aggregation of olivine formed directly from the solar nebula gas as recently proposed by Varela et al. (2005a). These objects constitute the products of the main condensation event, whereas BO chondrules represent the very early condensation of the major elements in the solar nebula that was capable of producing chondrule-sized liquid droplets.

If BO chondrules can form by the primary liquid condensation model, no second heating event is needed, and this eliminates one of the intriguing problems of chondrules formed by remelting of solids and partial evaporation, namely the lack of isotopic mass fractionation.

Whether or not there were cases where only solids or only a liquid condensed, the primary liquid condensation model can explain most observations and gives an answer to some of the questions regarding the origin of BO chondrules still left open by the melting of solid precursor model.

Acknowledgment

This paper benefit from the thorough reviews of Katharina Lodders and Roger Hewins and by the careful handling of the Chief Editor P. Nicholson. This study was supported by CONICET and SECyT (PICT 08176) in Argentina, FWF in Austria and NASA grant NNG04GG49G in the USA.

References

Alexander, C.M.O'D., 1996. Recycling and volatile loss in chondrule formation. In: Hewins, R.H., Jones, R.H., Scott, E.R.D. (Eds.), Chondrules and the Protoplanetary Disk. Cambridge Univ. Press, Cambridge, UK, pp. 233–242.

Alexander, C.M.O'D., 2004. Chemical equilibrium and kinetic constraints for chondrule and CAI formation conditions. Geochim. Cosmochim. Acta 68, 3943–3969.

Alexander, C.M.O'D., Grossman, J.N., Wang, J., Zanda, B., Bourot-Denise, M., Hewins, R.H., 2000. The lack of potassium-isotopic fractionation in Bishunpur chondrules. Meteorit. Planet. Sci. 35, 856–868.

Bischoff, A., Keil, K., 1984. Al-rich objects in ordinary chondrites: Related origin of carbonaceous and ordinary chondrites and their constituents. Geochim. Cosmochim. Acta 48, 693–709.

Blander, M., Katz, J.L., 1967. Condensation of primordial dust. Geochim. Cosmochim. Acta 31, 1025–1034.

Clayton, R.N., Onuma, N., Ikeda, Y., Mayeda, T., Hutcheon, I.D., Olsen, E.J., Molini-Velsko, C., 1983. Oxygen isotopic composition of chondrules in Allende and ordinary chondrites. In: King, E.A. (Ed.), Chondrules and Their Origins. Lunar & Planetary Institute, Houston, pp. 37–43.

Connolly, H.C., Jones, B.D., Hewins, R.H., 1998. The flash melting of chondrules: An experimental investigation into the melting history and physical nature of chondrule precursors. Geochim. Cosmochim. Acta 62, 2725–2735.

Dodd, R.T., 1978. The composition and origin of large microporphyritic chondrules in the Manych (L-3) chondrite. Earth Planet. Sci. Lett. 39, 52–66.

Ebel, D., Grossman, L., 2000. Condensation in dust-enriched systems. Geochim. Cosmochim. Acta 64, 339–366.

Givargizov, E.I., 1987. Highly Anisotropic Crystals. Reidel, Dordrecht, 394 pp.

Grossman, J.N., 1988. Formation of chondrules. In: Kerridge, J.F., Mathews, M.S. (Eds.), Meteoritics and the Early Solar System. Univ. of Arizona Press, Tucson, pp. 680–696.

Grossman, J., Wasson, J.T., 1982. Evidence of primitive nebular components in chondrules from the Chainpur chondrite. Geochim. Cosmochim. Acta 46, 1081–1099.

Grossman, J.N., Wasson, J.T., 1983a. Refractory precursor components of Semarkona chondrules and the fractionation of refractory elements among chondrules. Geochim. Cosmochim. Acta 47, 759–771.

Grossman, J.N., Wasson, J.T., 1983b. The composition of chondrules in unequilibrated chondrites: An evaluation of models for the formation of chondrules and their precursor material. In: King, E.A. (Ed.), Chondrules and Their Origins. Lunar & Planetary Institute, Houston, pp. 88–121.

Herndon, J.M., Suess, H.E., 1977. Can the ordinary chondrites have condensed from a gas phase? Geochim. Cosmochim. Acta 41, 233–236.

Hewins, R.H., 1988. Experimental studies of chondrules. In: Kerridge, J.F., Mathews, M.S. (Eds.), Meteorites and the Early Solar System. Univ. of Arizona Press, Tucson, pp. 660–679.

Hewins, R.H., 1989. The evolution of chondrules. Proc. Natl. Inst. Polar Res. Sympos. Antarct. Meteorites 2, 202–222.

Hewins, R.H., Fox, G.E., 2004. Chondrule textures and precursor grain size: An experimental study. Geochim. Cosmochim. Acta 68, 917–926.

Humayun, M., Clayton, R.N., 1995. Potassium isotope cosmochemistry: Genetic implications of volatile element depletion. Geochim. Cosmochim. Acta 61, 4689–4704.

Jones, R.H., Leshin, L.A., Guan, Y., Sharp, Z.D., Durakiewicz, T., Schilk, A., 2004. Oxygen isotope heterogeneity in chondrules from the Mokoia CV3 carbonaceous chondrite. Geochim. Cosmochim. Acta 68, 3423–3438.

Krot, A.N., Rubin, A.E., 1993. Chromite-rich mafic silicate chondrule in ordinary chondrites: Formation by impact melting. Meteorit. Planet. Sci. 24, 827–828. Abstract.

Kurat, G., 1988. Primitive meteorites: An attempt towards unification. Philos. Trans. R. Soc. London A 325, 459–482.

Kurat, G., Kracher, A., 1980. Basalts in the Lancé carbonaceous chondrite. Z. Naturforsch. 35a, 180–190.

Kurat, G., Varela, M.E., Hoppe, P., Clocchiatti, R., 1997. Glass inclusions in Renazzo olivine: Condensates from the solar nebula? Meteorit. Planet. Sci. 32. Abstract 76.

Kurat, G., Varela, M.E., Zinner, E., Engler, A., 2004. Condensation model for chondrules. Meteorit. Planet. Sci. 39. Abstract 57.

Lodders, K., Fegley, B., 2003. The Planetary Scientist Companion. Oxford Univ. Press, Oxford, UK, 371 pp.

Lofgren, G.E., 1989. Dynamic crystallization experiments on chondrule melts of porphyritic olivine composition: Textures experimental and natural. Geochim. Cosmochim. Acta 53, 461–470.

Lofgren, G.E., Lanier, A.B., 1990. Dynamic crystallization study of barred olivine chondrules. Geochim. Cosmochim. Acta 54, 3537–3551.

Lofgren, G.E., Russel, W.J., 1985. Dynamic crystallization experiments on chondrule melts of porphyritic olivine composition. Lunar Planet. Sci. 16, 499–500.

Lux, G., Keil, K., Taylor, G.J., 1981. Chondrules in H3 chondrites: Textures, compositions and origins. Geochim. Cosmochim. Acta 45, 675–685.

Matsuda, H., Nakamura, N., Noda, S., 1990. Alkali (Rb/K) abundances in Allende barred-chondrules: Implications for the melting conditions of chondrules. Meteoritics 25, 137–143.

McSween, H.Y., 1977. Petrographic variations among carbonaceous chondrites of the Vigarano type. Geochim. Cosmochim. Acta 41, 1777–1790.

McSween, H.Y., 1985. Constraints on chondrule origins from petrology of isotopically characterized chondrules in the Allende meteorite. Meteoritics 20, 523–540.

Métrich, N., Clocchiatti, R., 1989. Melt inclusions investigation of the volatile behaviour in historic basaltic magmas of Etna. Bull. Volcanol. 51, 185–198.

Nagahara, H., 1983. Texture of chondrules. Mem. NIPR Spec. Issue 30, 61–83.

Nitsan, U., 1974. Stability field of olivine with respect to oxidation and reduction. J. Geophys. Res. 79, 706–711.

Nuth III, J.A., Rietmeijer, F.J.M., Hill, H.G., 2002. Condensation process in astrophysical environments: The composition and structure of cometary grains. Meteorit. Planet. Sci. 37, 1579–1590.

Radomsky, P.M., Hewins, R.H., 1987. Dynamic crystallization experiments on an average type-I (MgO-rich) chondrule composition. Lunar Planet. Sci. 18, 808–809.

Radomsky, P.M., Hewins, R.H., 1990. Formation condition of pyroxene-olivine and magnesian olivine chondrules. Geochim. Cosmochim. Acta 54, 3475–3490.

Rietmeijer, F.J.M., Nuth III, J.A., Nelson, R.N., 2002. Laboratory hydration of condensed magnesiosilica smokes with implications for hydrated silicates in IDPs and comets. Meteorit. Planet. Sci. 39, 723–746.

Sears, D.W.G., Huang, S., Benoit, P.H., 1996. Open-system behavior during chondrule formation. In: Hewins, R.H., Jones, R.H., Scott, E.R.D. (Eds.), Chondrules and the Protoplanetary Disk. Cambridge Univ. Press, Cambridge, UK, pp. 221–232.

Suess, H.E., 1949. Zur Chemie der Planeten und Meteoritenbildung. Z. Elektrochem. 53, 237–241.

Tsuchiyama, A., Nagahara, H., Kushiro, I., 1980. Experimental reproduction of textures of chondrules. Earth Planet. Sci. Lett. 48, 155–165.

Tsuchiyama, A., Nagahara, H., Kushiro, I., 1981. Volatilization of sodium from silicate melt spheres and its application to the formation of chondrules. Geochim. Cosmochim. Acta 45, 1357–1367.

Tsuchiyama, A., Osada, Y., Nakano, T., Uesugi, K., 2004. Experimental reproduction of classic barred olivine chondrules: Open-system behavior of chondrule formation. Geochim. Cosmochim. Acta 68, 653–672.

Varela, M.E., Kurat, G., 2004. Glasses in meteorites. A unification model. Meteorit. Planet. Sci. 39. Abstract 109.

Varela, M.E., Kurat, G., Hoppe, P., Brandstätter, F., 2002. Chemistry of glass inclusions in olivines of the CR chondrite Renazzo, Acfer 182, and El Djouf 001. Geochim. Cosmochim. Acta 66, 1663–1679.

Varela, M.E., Kurat, G., Zinner, E., Métrich, N., Brandstätter, F., Ntaflos, T., Sylvester, P., 2003. Glasses in the D'Orbigny angrite. Geochim. Cosmochim. Acta 67, 5027–5046.

Varela, M.E., Kurat, G., Zinner, E., 2005a. A liquid-supported condensation of major minerals in the solar nebula: Evidence from glasses in the Kaba CV3 chondrite. Icarus 178, 553–569.

Varela, M.E., Kurat, G., Zinner, E., 2005b. Can glasses help us to unravel the origin of BO chondrules? Lunar Planet. Sci. XXXVI. Abstract 1436.

Weisberg, M.K., 1987. Barred olivine chondrules in ordinary chondrites. J. Geophys. Res. 92, E663–E678.

Wood, J., 1962. Chondrules and the origin of the terrestrial planets. Nature 197, 127–130.

Yoneda, S., Grossman, L., 1995. Condensation of CaO–MgO–Al_2O_3–SiO_2 liquids from cosmic gases. Geochim. Cosmochim. Acta 59, 3413–3444.

Yu, Y., Wang, J., Zanda, B., Alexander, C.M.O'D., Bourot-Denise, M., Hewins, R.H., 1998. Mass fractionation of K isotopes in chondrule evaporation experiments. Lunar Planet. Sci. XXIX. Abstract 1642.

Zinner, E., Crozaz, G., 1986. A method for the quantitative measurement of rare Earth elements in the ion microprobe. Int. J. Mass Spectrom. Ion Process. 69, 17–38.